What is Missing from the Prescription of Hydrology for Land Surface Schemes?

BRUCE DAVISON,[a,f] ALAIN PIETRONIRO,[b] VINCENT FORTIN,[c] ROBERT LECONTE,[d] MOGES MAMO,[e] AND M. K. YAU[a]

[a] *McGill University, Montreal, Quebec, Canada*
[b] *Environment and Climate Change Canada, Saskatoon, Saskatchewan, Canada*
[c] *Environment and Climate Change Canada, Montreal, Quebec, Canada*
[d] *Université de Sherbrooke, Sherbrooke, Quebec, Canada*
[e] *University of Saskatchewan, Saskatoon, Saskatchewan, Canada*

(Manuscript received 10 September 2015, in final form 15 February 2016)

ABSTRACT

Land surface schemes (LSSs) are of potential interest both to hydrologists looking for innovative ways to simulate river flow and the land surface water balance and to atmospheric scientists looking to improve weather and climate predictions. This paper discusses three ideas, which are grounded in hydrological science, to improve LSS predictions of streamflow and latent heat fluxes. These three possibilities are 1) improved representation of lateral flow processes, 2) the appropriate representation of surface heterogeneity, and 3) calibration to streamflow as a way to account for parameter uncertainty. The current understanding of lateral hydrological processes is described along with their representation of a selected group of LSSs. Issues around spatial heterogeneity are discussed, and calibration in hydrologic models and LSSs is examined. A case study of an evapotranspiration-dominated basin with over 10 years of extensive observations in central Canada is presented. The results indicate that in this particular basin, calibration of streamflow presents atmospheric modelers with a unique opportunity to improve upon the current practice of using lookup tables to define parameter values. More studies are needed to determine if model calibration to streamflow is an appropriate method for generally improving LSS-modeled heat fluxes around the globe.

1. Introduction

Land surface schemes (LSSs) were first developed for large-scale climate applications in general circulation models (GCMs) in the late 1960s (Manabe 1969). Subsequent developments in LSS equations representing physical processes from very simple models to more sophisticated 1D vertical models of vegetation, soil, snow, surface temperature, and moisture are summarized by Sellers et al. (1997a), Pitman (2003), Yang (2004), and Niu and Zeng (2012). Until recently, however, land surface model developers have not attempted to incorporate surface heterogeneity or a variety of processes representing horizontal hydrological fluxes such as the surface movement of snow and water, the subsurface movement of water, river flow, and human influences (Koster et al. 2000; Livneh et al. 2010; Niu and Zeng 2012), nor appropriately made use of methods to manage land surface parameter uncertainty (Bastidas et al. 2006; Samaniego et al. 2010; Mendoza et al. 2015). These challenges, which can be managed using well-established methods in hydrology, have limited the usability of LSSs for hydrological applications and handicapped LSSs for their original purpose of providing accurate lower-boundary conditions for atmospheric models. This paper examines some of the ways in which the science of hydrology and techniques of hydrological modeling are being applied to LSSs to improve their simulations of latent heat flux to the atmosphere and suggests some things to consider when working to improve the application of LSSs for hydrological and atmospheric prediction.

Streamflow measurements provide a unique opportunity for LSS modelers because rivers provide an integrated response to hydrological processes throughout

[f] Current affiliation: Environment and Climate Change Canada, Saskatoon, Saskatchewan, Canada.

Corresponding author address: Bruce Davison, Environment and Climate Change Canada, 11 Innovation Blvd., Saskatoon, SK S7N 3H5, Canada.
E-mail: bruce.davison@canada.ca

DOI: 10.1175/JHM-D-15-0172.1

the landscape. With few exceptions, and as will be discussed, recent efforts to incorporate appropriate physical processes, surface heterogeneity, and parameter uncertainty in LSSs are incomplete. To improve the utility of LSSs for hydrologic and atmospheric modeling, it is the purpose of this paper to suggest a path forward to overcome some fundamental inadequacies of the LSSs and how they are employed. Overcoming these challenges is particularly important if the LSS development community wants to convince water managers that LSSs can provide better results than traditional distributed hydrologic models. Specifically, this paper examines the following:

1) how some of the more sophisticated LSSs deal with the lateral flow of water (channel, land surface, subsurface, and human influenced),
2) some important issues around surface heterogeneity, and
3) calibration of streamflow as an approach to account for parameter uncertainty for atmospheric and hydrologic prediction.

The ideas presented here share much in common with the concepts presented by Clark et al. (2015a), who make the same claim that Earth system models (ESMs; of which LSSs are an important subset) have much to gain from collaborating with hydrologists to incorporate hydrological modeling concepts and observations in the drive to improve ESMs. The focus of this paper, however, more narrowly concentrates on lateral hydrological processes in LSSs and presents a case study to exemplify some of the potential for LSSs that include more sophisticated hydrological understanding in the modeling framework.

The case study examined is in the White Gull Creek basin in central Saskatchewan, Canada, and explores issues around lateral flow processes, surface heterogeneity, and parameter uncertainty. The case study is done using the Canadian Land Surface Scheme (CLASS; Verseghy 1991; Verseghy et al. 1993) within the hydrologic–land surface modeling platform Modélisation Environmentale Communautaire (MEC)–Surface and Hydrology (MESH; Pietroniro et al. 2007).

2. Understanding lateral hydrological processes in nature

The literature reveals a number of important lateral hydrological processes. These processes include overland flow, interflow, groundwater flow, river routing, blowing snow redistribution, wetland dynamics, lake routing, reservoir routing, streamflow diversions and interbasin transfers, irrigation, and human-induced surface and subsurface drainage.

Overland flow has traditionally been described as infiltration excess (Horton 1933) or saturation excess (Dunne and Black 1970a,b). In the first case, rainfall or snowmelt exceeds the capacity of the soil to absorb the water. In the second case, the soil becomes saturated and is unable hold any more water. The result in both cases is overland flow. Dunne (1978) provides a comprehensive description of both types of overland flow. Spence (2010), however, describes a paradigm shift in thinking with respect to runoff generation from hillslopes to basin outlets. The idea that contributing areas change in size in a continuous manner to produce runoff is being challenged by a multitude of field studies that illustrate the dominance of threshold-mediated and connectivity-controlled processes in runoff production. These threshold and connectivity boundary conditions are dictated by the heterogeneity in the basin (Spence 2010) and are impossible to explicitly map and incorporate into models (McDonnell et al. 2007).

In addition to infiltration excess and saturation excess overland flow, a third runoff process is prevalent in the hillslope hydrology literature. Interflow is a term that is often used interchangeably with subsurface storm flow, lateral flow, subsurface runoff, transient groundwater, soil water flow, throughflow, unsaturated Darcian flow in the soil matrix, or pipe flow in macropores (Weiler et al. 2005; Dingman 1994, p. 421). To further complicate matters, the same term is sometimes used to describe slightly different processes. Here, interflow is defined as the lateral flow of water between the soil surface and above the water table. The water table is defined as the surface at atmospheric pressure within the soil profile.

Spence (2010) and McDonnell (2003, 2013) highlight the need for new modeling approaches if the findings of field (hillslope) hydrologists are to be incorporated into "physically based" hydrological models. McDonnell (2003) states that one of the most notable paradigm shifts results from the finding that pre-event water dominates storm hydrographs, which questions the fundamental assumptions underlying dominant theories and model representations of overland flow. Spence (2010) emphasizes another paradigm shift in understanding runoff generation processes, from theories relying on runoff generation and variable contributing area as a continuum to an understanding based on thresholds that depend on the interconnections between different parts of the landscape. The similarities between overland flow and subsurface storm flow add further complications. Similar to threshold and connectivity processes for overland flow, McDonnell (2013) highlights similarities for subsurface flow. Some hillslopes experience fill-and-spill flow at the subsurface soil–bedrock interface. Other hillslopes experience rapid lateral flow when the water table rises into more transmissive layers. Whereas overland flow

threshold and connectivity processes are theoretically possible to study using remote sensing techniques, similarly examining subsurface thresholds and connectivity becomes much more complex.

Briefly touched upon in many papers on the topic of hillslope hydrology, groundwater also plays an important role in many rivers. In this paper, groundwater refers to the water in the soil below the water table, and the lateral flow of groundwater to streams is referred to as base flow. The pioneering textbook by Freeze and Cherry (1979) goes into detail about the physical laws describing groundwater flow. Recent modeling studies also highlight the increasing evidence that groundwater influences weather and climate (Maxwell and Kollet 2008; Miguez-Macho and Fan 2012a,b). One global estimate of water-table depth suggests that 15% of the global land area feeds surface water and an additional 7%–17% of the global land area has a water table or capillary fringe that is accessible to plant roots (Fan et al. 2013). Field studies illustrate that groundwater can keep peatlands wet to maintain base flow and control summer rain responses in dry conditions (Branfireun and Roulet 1998). Two-way interaction between streams and groundwater is also an important process influencing the overall water cycle. For example, floodwaters are important sources of recharge in many parts of the world (e.g., Taylor et al. 2013) and, at least in the groundwater modeling community, it is well known that rivers and other water bodies strongly influence the groundwater table (Harbaugh et al. 2000). Of interest to LSS modelers is the possibility of using confined aquifers to monitor large-scale water balance changes (Marin et al. 2010).

River routing is concerned with the movement of water within an open channel. The physics underlying river-routing models and open-channel hydraulics has been well understood for decades (Chow 1959). One area of research where the physics of river routing is still being illuminated is the phenomenon of ice jamming, which can cause disastrous floods in very short periods of time. Although progress is being made with respect to understanding a variety of physical processes related to ice jamming, there are still major unknowns related to the formation and release of ice jams (Beltaos 2008). Recent research initiatives related to river routing also include links to our understanding of ecosystems (e.g., Morin et al. 2003; Mingelbier et al. 2008). However, perhaps of more immediate interest to LSS modelers are the recent and expected advances in estimating river characteristics and model parameters that allow for more sophisticated river-routing approaches to be used [as described in appendix A5 of Clark et al. (2015a)].

Blowing snow redistribution can be an important process affecting the flow patterns of rivers (Fang and Pomeroy 2009; MacDonald et al. 2009). In winter, wind can move large amounts of snow from open areas to vegetated areas or other sheltered areas of low wind, such as the leeward sides of hillslopes (Vionnet et al. 2014). This process often occurs at the subgrid scale of global hydrological models (GHMs) or LSSs.

Wetlands also have considerable influence on streamflow. Sheet flow and channel flow over a wetland surface or water exchanges with upland systems can affect streamflow by changing the nature of the storage and release of water between wetlands and streams (Price and Waddington 2000).

In many parts of the world, lakes and rivers are intimately connected (Jones 2010). Streams are not always long, continuous ribbons of water that drain watersheds, and they often contain many small or large lakes within the river–lake system. The percentage of a watershed covered by lakes, the position of the lakes within a watershed, the percentage of river kilometers flowing through lakes or rivers, and the size distribution of lakes will all influence the flow of water in a stream–lake network (Jones 2010).

In addition to the natural lateral hydrological processes described above, humans often have a direct impact on the lateral movement of water on the land surface. As summarized below, Nazemi and Wheater (2015a,b) provide a detailed survey of the human management of water in terms of water demand and water supply and their representation in GHMs and LSSs.

Water demand is characterized as irrigative or nonirrigative. Irrigation accounts for the vast majority of surface and groundwater extractions that evaporate to the atmosphere, thus being effectively removed from the basin and river system unless precipitation brings this water back into the basin. Nonirrigative demands include municipal, industrial, and agricultural uses that return flow to the basin. In many communities, for example, municipal water is extracted, used by people, and then returned to the environment without evaporating much water to the atmosphere. Nonirrigative uses, however, can alter the water quality and timing of water movement within a basin.

Nazemi and Wheater (2015a,b) characterize water supply as the means by which water is extracted and stored to meet human demands. These means include the use of reservoirs, streamflow diversions and interbasin transfers, groundwater extraction, and desalination and water reuse. In addition to the methods described by Nazemi and Wheater (2015a,b) of extracting and storing water for use, water supply issues include the artificial drainage of water for human endeavors. An example of a common practice that can have a large impact on some watersheds is agricultural

TABLE 1. List of LSSs considered in this review, their host institutions, and primary references.

Model acronym	Full model name	Host institution	References
CLM4	Community Land Model, version 4	NCAR, United States	Lawrence et al. (2011)
Noah	Noah	NCEP, United States	Mitchell (2005); Niu et al. (2011)
HTESSEL	Hydrology Tiled ECMWF Scheme of Surface Exchanges over Land	ECMWF, United Kingdom	Balsamo et al. (2009); Pappenberger et al. (2010)
CLSM	Catchment Land Surface Model	NASA GMAO, United States	Koster et al. (2000)
JULES	Joint UK Land Environment Simulator	Met Office, United Kingdom	Best et al. (2011)
ISBA	Interactions between Soil, Biosphere, and Atmosphere	Centre National de Recherches Météorologiques (CNRM), Météo-France, France	Decharme et al. (2012)
VIC	Variable Infiltration Capacity model	University of Washington, United States	Liang et al. (1994)
MESH (CLASS)	Canadian Land Surface Scheme (CLASS) within the hydrologic–land surface modeling platform Modélisation Environmentale Communautaire (MEC)–Surface and Hydrology	Environment and Climate Change Canada, Canada	Pietroniro et al. (2007)
MATSIRO	Minimal Advanced Treatments of Surface Interaction and Runoff	University of Tokyo, Japan	Takata et al. (2003)

drainage (Schottler et al. 2014), which includes surface water drainage and subsurface tile drainage in agricultural areas.

For the purposes of considering how LSSs consider lateral fluxes of water for hydrological modeling purposes, the human influences that are considered include irrigation and drainage on the demand side and reservoirs, diversions, and interbasin transfers on the supply side. Although nonirrigative water demands can have an influence on the water cycle, these influences are often the result of reservoir operations. Groundwater extraction can also have an influence on streamflow, but it is considered beyond the scope of this paper.

3. Brief comparison of lateral hydrology in LSSs

A number of LSSs that include lateral hydrology [hereafter referred to as hydrologic LSSs (H-LSSs)] are being developed in the research community, as reflected in the literature. A large number of LSSs are in existence, and numerous studies have been done to compare their capabilities in different circumstances (e.g., Henderson-Sellers et al. 1995; Boone et al. 2004). For the purposes of brevity, only nine H-LSSs were considered for this review. These H-LSSs include the Variable Infiltration Capacity model (VIC), which has been utilized as both a hydrological model and an LSS (Gao et al. 2009). The H-LSS MESH (Pietroniro et al. 2007) is also included, as it is most familiar to the authors and is used in the case study. The remainder of the H-LSSs considered were selected based on our subjective evaluation of how much information could be found in the scientific literature. Table 1 lists the H-LSSs, the full name of each model, their host institutions, and primary references. Seven of the LSSs considered correspond with the 11 LSMs considered in Clark et al. (2015a). Two LSSs that are included in this publication, ISBA and MESH, have particular importance in Canada. ISBA is the LSS of Canada's Global Environmental Multiscale (GEM) numerical weather prediction (NWP) model (Bélair et al. 2003a,b). This version of ISBA is currently undergoing a major revision, and the resulting LSS is being renamed the Soil, Vegetation and Snow (SVS) scheme (Alavi et al. 2016; Husain et al. 2016). MESH is an alternative research-based modeling platform that is being developed in Canada and currently includes CLASS as the LSS.

Table 2 shows which models represent which hydrologic processes in this brief comparison of H-LSSs. It is possible that some process improvements are currently being studied in some H-LSSs of which the authors are unaware. Only lateral fluxes are considered. For example, Bowling et al. (2004) describe the implementation of blowing snow within VIC, but the algorithm only affects sublimation rates rather than blowing snow redistribution on the landscape, so it is not considered here.

Table 2 is similar to Table 2 of Clark et al. (2015a), but as already noted, with a focus on lateral hydrological processes rather than the overall water budget. This emphasis on lateral processes highlights certain aspects of the water budget that are not considered in detail by Clark et al. (2015a), such as blowing snow redistribution; wetland dynamics; differences between river routing and lake or reservoir routing; and human influences related to reservoirs, streamflow diversions, interbasin transfers, irrigation, and human-induced surface and

TABLE 2. List of references for selected lateral hydrologic processes used in, or linked to, the chosen LSSs. For overland and groundwater flow, the type of approach is listed as a probability distribution function of topographic characteristics (top), soil storage (ss), or other (oth).

Lateral hydrologic processes	CLM4	Noah	HTESSEL	CLSM	JULES	ISBA	VIC	MESH	MATSIRO
Overland flow	(top) Niu et al. (2005)	(top) Niu et al. (2011); (ss) Mitchell (2005); Schaake et al. (1996)	(ss) Balsamo et al. (2009)	(top) Koster et al. (2000)	(top or ss) Best et al. (2011)	(top) Decharme et al. (2012); (ss) Habets et al. (1999)	(ss) Liang et al. (1996)	(oth) Soulis et al. (2000); PDMROF, Mekonnen et al. (2014)	(top) Takata et al. (2003)
Interflow	—	—	—	—	—	—	—	Soulis et al. (2000)	—
Groundwater flow	(top) Niu et al. (2005)	(top) Niu et al. 2011; (ss) Mitchell (2005)	(ss) Pappenberger et al. (2010)	(top) Koster et al. (2000)	(top or ss) Best et al. (2011)	(ss) Habets et al. (1999); Vergnes et al. (2012)	(ss) Liang et al. (1996)	(oth) Soulis et al. (2000)	(top) Takata et al. (2003)
River routing	Oleson et al. (2010)	Gochis et al. (2013)	Pappenberger et al. (2010)	—	Zulkafli et al. (2013)	Decharme et al. (2012)	Lohmann et al. (1996, 1998)	Soulis et al. (2000)	Pokhrel et al. (2012)
Blowing snow redistribution	—	—	—	—	—	Vionnet et al. (2014)	—	MacDonald et al. (2009); MacDonald (2010)	—
Wetland dynamics	Oleson et al. (2010)	—	—	—	—	Decharme et al. (2012)	Bowling and Lettenmaier (2010)	—	—
Lake routing	Oleson et al. (2010)	—	—	—	—	—	Bowling and Lettenmaier (2010)	Kouwen and Mousavi (2002)	—
Reservoir routing	Voisin et al. (2013b)	—	—	—	—	—	Voisin et al. (2013a)	Kouwen and Mousavi (2002)	Pokhrel et al. (2012)
Streamflow diversions and interbasin transfers	—	—	—	—	—	—	—	—	—
Irrigation	Voisin et al. (2013b)	—	—	—	—	—	Voisin et al. (2013a)	—	Pokhrel et al. (2012)
Surface and subsurface drainage	—	—	—	—	—	—	—	—	—

subsurface drainage. Table 2 is included here to highlight the gaps in the incorporation of lateral hydrology in many LSSs. Appendix A in this publication includes, in a parallel manner to appendix A in Clark et al. (2015a), a description of the overall water budget for CLASS, MESH, ISBA, and SVS.

4. Some important issues around spatial heterogeneity and parameterization

Hydrologic and land surface modelers have approached the challenge of land surface heterogeneity in a variety of ways. Heterogeneity comes in many forms, such as variable atmospheric forcing, vegetation type, elevation, slope, aspect, and soil moisture (Leavesley and Stannard 1990; Ghan et al. 1997). These heterogeneities can impact how the land surface partitions fluxes of energy, mass, and momentum across the landscape and to the atmosphere through a range of spatial scales (Ke et al. 2013).

One way to classify modeling approaches is to categorize them by how they deal with the challenge of spatial heterogeneity. The lexicon of spatial heterogeneity in (not purely statistical) hydrological modeling usually refers to distributed, semidistributed, and lumped models (e.g., Becker 1992; Karvonen et al. 1999; Jajarmizadeh et al. 2012). Distributed modeling can be further subdivided into distributed integral and distributed differential models (Todini 1988).

The remainder of this section describes some key considerations in accounting for spatial heterogeneity; ties these considerations to the overarching topics of hierarchical spatial organization and model complexity, agility, efficiency, and fidelity; and compares how spatial heterogeneity is accounted for in hydrologic models and land surface schemes.

a. Key considerations related to spatial heterogeneity

Spatial heterogeneity complicates the mathematical modeling of land surface processes and makes it rather challenging to accurately describe the subtleties of how a modeler must make decisions about how to represent the landscape. There are key questions for a modeler to consider:

- How much does the model know about the spatial location of different parts of the land surface?
- How is the lateral movement of water and energy represented?
- What is the a priori knowledge of parameter values and state variables?
- How much area should each land surface unit represent?
- Which sub-land-surface units should vary dynamically?

In an attempt to clarify the subtle choices a modeler must make when representing spatial heterogeneity, each of these questions is explored.

First, the language of lumped, distributed, and semidistributed modeling refers to how much the model knows about the spatial location of various features on the landscape. In a lumped model, the spatial locations of subunits of the landscape are not known, whereas in distributed modeling their locations are identified. In a semidistributed model, the locations of units (i.e., grid cells or polygons) of a certain size are known, while the locations of subunits of the landscape are lumped together whether or not their locations are known.

Second, with respect to representing the lateral movement of water and energy, Clark et al. (2015b) clarify the classification of distributed integral and distributed differential models by Todini (1988). Distributed integral models are a spatial collection of independent 1D vertical column models interacting laterally only by the inclusion of a digital river network while distributed differential models explicitly simulate all lateral fluxes between the distributed model elements. Unfortunately, there does not appear to be standard terminology for one additional way of representing the lateral movement of water and energy. It is possible to represent fluxes between multiple grouped land surface elements in a lumped or semidistributed model. Although uncommon, examples of this subunit lateral flux include blowing snow from one land type to another in MacDonald (2010) and lateral subsurface flow between two land surface types depicted in Fig. 2c of Clark et al. (2015b).

Third, the a priori knowledge of parameter values and state variables has a direct impact on how they should be spatially represented in the model (Todini 1988). Stochastic parameterizations should be used when little is known about the parameter values, and physical parameterizations should be used when there is a priori knowledge of parameter values.

Fourth, the area represented by each land surface unit (grid cell or polygon) is very important to consider. The increasing availability of high-resolution spatial data combined with the increasing power of computers is giving hydrologic and LSS modelers the capability to model continental domains at higher resolutions than previously possible [as discussed by Wood et al. (2011), Beven and Cloke (2012), Bierkens et al. (2015), and Archfield et al. (2015)]. However, to model large areas at such hyperresolutions still requires relatively sophisticated hardware. In addition, some heterogeneous land surface characteristics (such as elevation) are easier to measure than others (such as soil moisture and hydraulic conductivity), and this presents a significant challenge

for modeling at any resolution, but particularly for hyperresolution model configurations. Even at resolutions on the order of 1 m, surface heterogeneity can be significant. The primary author of this paper has participated in soil moisture field campaigns and personally measured significant differences in soil moisture measurements taken at locations within centimeters from one another. In addition, the representation of many physical processes is based on theories that are developed using measurements at one spatial and temporal scale, and then applied within a model at a different spatial or temporal resolution. For example, the calculation of sensible and latent heat fluxes at the surface–atmosphere interface are 1D vertical calculations in an LSS, which may not be appropriate with small grids given lateral fluxes of these variables at smaller scales (e.g., Neumann and Marsh 1998). The challenge that results from the scale mismatch between theory and practice in a model is in understanding how to parameterize spatially heterogeneous processes within model grid cells (Beven 1996).

Finally, it is important to consider if the sub-land-surface units should vary dynamically. One example of this consideration is in situations where land surface change is occurring during the simulation period. If the sub-land-surface units are based on vegetation and forested areas have been harvested or burned, this land surface change may be important to incorporate into the modeling effort.

b. *The connection between hierarchical spatial organization and spatial heterogeneity*

Whether talking about lumped, distributed, or semidistributed models, there exists a natural hierarchical spatial organization to representing spatial heterogeneity. In short, the locations of larger land units are known, while the locations of smaller subland units are lumped together regardless of the knowledge of their spatial location. Of course, as shown in Fig. 2bii of Clark et al. (2015b), the subunits of land can be discretized as spatially contiguous grid cells, which one might consider to be a nested distributed model. In Clark et al. (2015b), the larger units of land are called grouped response units (GRUs) and the smaller subunits of land are called hydrologic response units (HRUs). The use of the term GRU to describe response units that are distributed across the landscape in a contiguous manner represents a deviation from the long-standing use of the term GRU, which is essentially the same as an HRU. To avoid confusion, we advocate for the term distributed response unit (DRU) to be used to represent the larger land units in the hierarchical spatial nomenclature. For the smaller subunits that are lumped together, we recommend continuing to use the existing terms GRU (Kouwen and Mousavi 2002), HRU (Leavesley and Stannard 1990), and hydrologically similar unit (HSU; Karvonen et al. 1999). The only real difference between the GRU, HRU, and HSU is in how they are traditionally set up. At its core, they are all slightly different manifestations of the same approach to semidistributed modeling, albeit traditionally applied in different ways.

c. *Connections between model complexity, agility, efficiency, and fidelity*

The issues of surface heterogeneity are closely linked with issues around model complexity, fidelity, efficiency, and agility. Model complexity is defined by Clark et al. (2015a) to include "the extent to which physical processes are represented explicitly as well as the discretization and connectivity of the physical landscape." In essence, the key considerations described in section 4a define the model complexity, including the connection between the representation of physical processes and spatial heterogeneity. The agility of any particular model is determined by the model's ability to allow the modeler to make decisions about how much complexity to introduce to a particular modeling exercise, or by the modeler's ability to change the model structure or work with different models.

The decisions made by a modeler related to model complexity have a direct connection to model efficiency. In general, choices that result in added complexity will reduce the model efficiency. Unfortunately, the tradeoffs between model efficiency and model fidelity are not well understood and are incredibly important given that model complexity is increasing rapidly because of the incorporation of "a bewilderingly large set of processes" (Clark et al. 2015a) and hyperresolution modeling (Wood et al. 2011). Such increases to model complexity make it difficult to characterize uncertainty (e.g., using multiple ensemble members) and comprehensively perform parameter estimation experiments.

d. *How LSSs compare to hydrologic models when representing surface heterogeneity*

The methods of subgrid representation in LSSs fit within the conceptual realm of distributed integral or grid-based semidistributed hydrological models. Figure 1 is based on Fig. 2 of Boone et al. (2004), and the five tile classes are described as follows.

In tile type *A*, each grid cell can be composed of multiple tiles, but subgrid variability is not tracked from one time to the next, resulting in a single effective tile for each grid cell. Tile type *B* is similar to type *A*, except that one component of the energy balance is kept separate at the subgrid scale based on the characteristics of the tile.

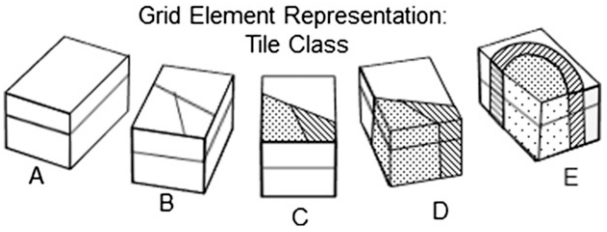

FIG. 1. Components of a hydrologic–land surface model grid cell, based on Fig. 2 of Boone et al. (2004). Tiles are classified as: single tile for each grid cell ("A"), only one component of the energy balance is tiled ("B"), only surface components are tiled ("C"), static tile fractions throughout the soil column in each grid cell ("D"), and tile fractions vary dynamically based on internal state variables and tiles vary throughout the soil column ("E").

Tile type *C* separates calculations of the surface variables and does not average them throughout the grid cell at the end of each time step. Tile type *D* maintains static percentages of each tile in each grid cell while calculating the column of variables without averaging them at the end of each time step. Tile type *E* separates calculations of the entire column of surface and subsurface variables without averaging them at the end of each time step, with the added complexity of each tile changing dynamically from one time to the next based on the value of a state variable.

Tile type *A* is equivalent to distributed integral hydrological modeling, whereas the remaining tile types are variations of grid-based semidistributed modeling. The GRU/HRU/HSU approach can easily be configured for tile types *A*, *B*, *C*, and *D*, as long as there is a mechanism to override the selected GRU/HRU/HSU parameter values with grid-based parameter values. Generally speaking, LSSs generate tiles with satellite-derived estimates of the spatial distribution of vegetation, although some LSS studies have also used elevation and vegetation to determine tiles for each grid cell (Ke et al. 2013).

5. Parameter estimation in hydrologic models and H-LSSs

Related to the challenges associated with how horizontal hydrological processes and surface heterogeneity are represented in hydrologic and LSS models, a number of major research challenges associated with parameter estimation are important to consider. These challenges include appropriately estimating a priori parameter values, reducing errors where incorrect parameter values compensate for other errors in the model cascade, and regionalizing parameters.

The LSS and hydrologic modeling communities have traditionally approached these challenges in fundamentally different ways. At one end of the spectrum, atmospheric modeling applications of LSSs tend to make use of static lookup tables for parameter values, relying on a priori parameter estimation techniques that typically use transfer functions that relate geophysical attributes to model parameters (Santanello et al. 2013; Archfield et al. 2015). At the other end of the spectrum, the hydrologic modeling community has been developing a wide variety of parameter estimation techniques using model simulations and available response data to quantify uncertain model parameters. These parameter estimation methods generate either a single parameter set or multiple parameter sets. The methods that generate a single parameter set can be viewed as model calibration methods that look for a single best solution, while the methods that generate multiple parameter sets look for parameter distributions rather than single-point estimates [for a brief review, see Matott et al. (2009)].

We are of the view that generating parametric ensemble distributions is generally superior to looking for single solutions through model calibration. However, given that operational atmospheric models generally use a priori parameter estimates, and given the relative ease of model calibration (when compared to generating multiple parameter sets), the case study presented in section 6 will compare an a priori parameter estimation to a single parameter set found by calibrating the model to measured streamflow. The results of the case study should be extensible to the generation of parametric ensembles when using parameter estimation techniques that look for parameter distributions rather than single solutions.

The remainder of this section provides a brief review of calibration in hydrologic models and H-LSSs.

Calibrating hydrologic models and LSSs

Calibration of hydrologic models has a long history, of which the first 40 years, from the first developments of computer-based hydrological models the early 1960s, is described by Gupta et al. (2003). The earliest methods of calibration were manual in nature, relying on the expertise of an experienced hydrologist who was knowledgeable about both the watershed of interest and the model being used to represent the basin. Automated calibration techniques started developing in the early 1970s, traditionally considering only one measure of closeness (called an objective function) between the observed and modeled streamflow.

Contemporary hydrologic model calibration often includes multiple objectives in the evaluation of trade-offs in water resources systems (Reed et al. 2013). Gupta et al. (1998) were the first to consider multiple objectives to highlight structural errors in a

hydrological model. Multiobjective calibration of hydrological models has since exploded in the scientific literature, as outlined in a review by Efstratiadis and Koutsoyiannis (2010). Despite the strong interest in multiobjective model calibration in the research community of hydrologic modelers, single objective calibration is still widely used.

The term ''calibration'' correctly gives the impression that the focus of the exercise is to tweak model parameters to achieve an optimal match between the simulation and observations, which inherently covers up other errors. Although model calibration may compensate for errors in various uncertain elements of the model (such as incorrect structure or forcing data), model parameter calibration can give a false assurance that a particular model and parameter set (or sets) can be used for predictive purposes in all circumstances.

In contrast to hydrologic modeling, calibration is relatively uncommon in LSSs, where the focus has primarily been on developing a priori parameter sets. A number of studies have been performed to optimize LSS parameters using observed state variables such as surface temperature and soil moisture (Gupta et al. 1999; Hess 2001; Hogue et al. 2005; Liu et al. 2003, 2004, 2005; Santanello et al. 2007; Peters-Lidard et al. 2008; Harrison et al. 2012; Santanello et al. 2013). One issue, however, with calibrating LSSs is that many important parameters are hard coded (Mendoza et al. 2015), which limits the models' abilities to replicate important hydrological processes.

In the Model Parameter Estimation Experiment (MOPEX), Duan et al. (2006) compared hydrological models and LSSs with respect to their ability to predict streamflow using a priori parameters and calibrated parameters. They concluded that calibration is required to accurately predict streamflow. According to Nasonova et al. (2009), the results from the MOPEX study showed that the hydrological models performed better than the LSSs, possibly because of better calibration of the hydrological models. Nasonova et al. (2009) and Xie et al. (2007) showed that an LSS could produce comparable streamflow simulations if calibrated effectively. More recently, Huang et al. (2013) performed a sensitivity analysis of parameters in CLM over 20 watersheds as a preliminary step to provide guidance in reducing the number of LSS parameters to calibrate for 431 MOPEX sites in the United States.

6. White Gull Creek case study

Using the MESH model, the case study presented here explores issues around the representation of hydrological processes, heterogeneity of the land surface, and calibration as a method of dealing with parameter estimation. The work presented in this case study has some similarities to one of the coauthor's master's thesis (Mamo 2015) but is fundamentally different.

a. Basin information

1) BASIN DESCRIPTION

White Gull basin (Fig. 2), the study site selected for this case study, is located 60 km northeast of Prince Albert, Saskatchewan, at the southern end of the Canadian boreal forest between latitudes 53.99° and 54.13°N and longitudes 104.62° and 105.08°W. The White Gull basin drains an effective area of 603 km^2. White Gull Lake, which covers an area of 26 km^2, is located at the southwest corner of the basin but is known to be noncontributing to the streamflow and is excluded from the drainage area and hydrological analyses.

The White Gull Creek basin falls on two ecological units called ecodistricts, which are based on relatively homogeneous biophysical and climatic conditions, regional landform, local surface form, permafrost distribution, soil development, textural group, vegetation cover/land-use classes, range of annual precipitation, and mean temperature (Ironside 1991). The two ecodistricts that intersect the basin are the Whiteswan Uplands and White Gull Plains (Fig. 2b). The Whiteswan Uplands (ecodistrict 658), covering the western portion of the basin, is characterized by poorly drained wetlands with thick, low-permeability, clay-rich glacial till deposits and a shallow groundwater table. The groundwater fluctuates from the surface to about 1.5 m below ground surface (Judd-Henrey et al. 2008; van der Kamp and Hayashi 2009). In contrast, the eastern side of the basin, White Gull Plains (ecodistrict 659), is moderately to well drained with sand and gravel outwash and a deeper groundwater table of 5–10 m.

Vegetation cover of the basin consists of aspen, spruce, tamarack, and jack pine, with some deciduous trees. Old black spruce is the dominant vegetation cover in the western portion of the basin (Whiteswan Uplands ecodistrict), while mature jack pine is the main vegetation cover in the eastern part of the basin (White Gull Plains ecodistrict; Barr et al. 2012; Nijssen and Lettenmaier 2002).

White Gull basin has a history of intensive observations that began with the Southern Study Area (SSA) of the Boreal Ecosystem–Atmosphere Study (BOREAS) in 1993 (Sellers et al. 1997b). Two sites of intensive observations in White Gull basin are the old black spruce (OBS) site and the old jack pine (OJP) site (ORNL DAAC 2015). Water balance estimates of these sites were performed by Barr et al. (2012) for the hydrologic year (October–September) using the equation $O = P - \mathrm{ET} - \Delta S$,

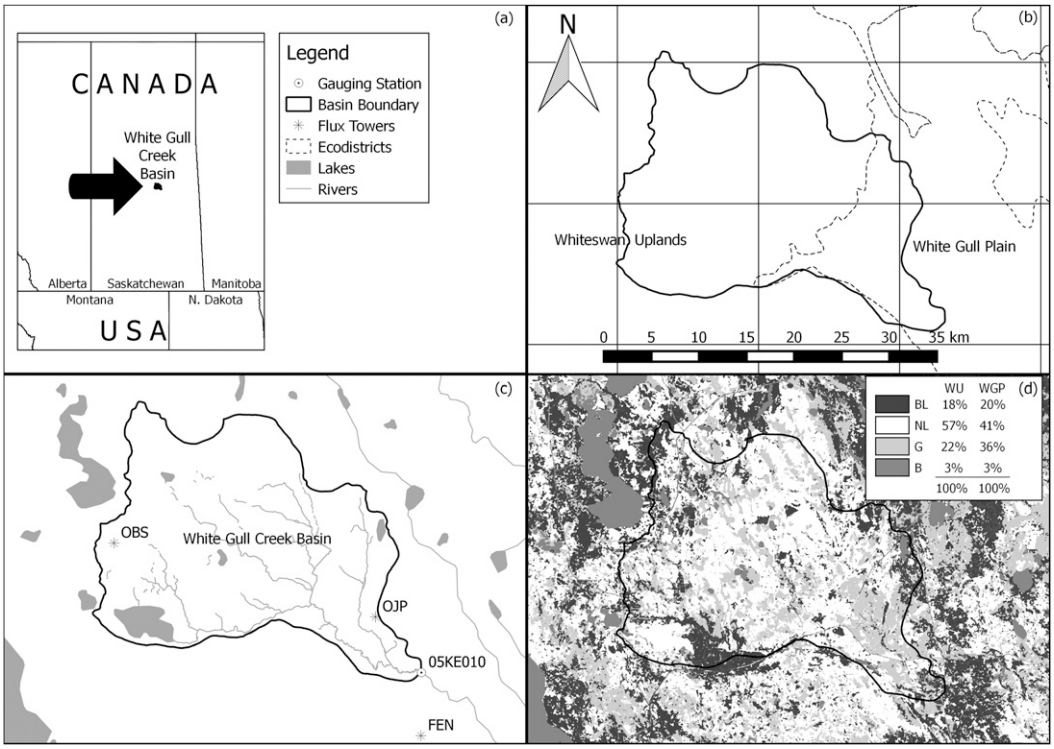

FIG. 2. (a) Location of White Gull Creek in Canada; (b) model grid, basin, and ecodistrict boundaries; (c) river network, streamflow gauge, and flux towers; and (d) land cover. The percentages of land cover in Whiteswan Uplands (WU) and White Gull Plains (WGP) are listed in (d) [broadleaf forest (BL), needleleaf forest (NL), grass (*G*), and barren (*B*)].

where O represents stand-level outflow and P, ET, and ΔS are the measured precipitation, evapotranspiration, and change in storage terms, respectively. When energy closure is considered for the evapotranspiration term, the OBS site had a mean annual precipitation of 491 mm yr^{-1}, evapotranspiration of 382 mm yr^{-1}, change in storage of 2 mm yr^{-1}, and outflow of 108 mm yr^{-1} for the years 1999–2009. Similarly, the OJP site had a mean annual precipitation of 527 mm yr^{-1}, evapotranspiration of 306 mm yr^{-1}, change in storage of 34 mm yr^{-1}, and outflow of 187 mm yr^{-1} for the years 2002–09. When scaled up to the watershed, these calculations of outflow aligned very well with the streamflow measurements of White Gull Creek. As a result, it is very clear that the evapotranspiration is a dominant component of the water balance when compared to the lateral flows, which has implications in interpreting the modeling results.

2) BASIN DATA

MESH requires physiographic data for setting up and parameterizing the model and meteorological data for driving the model. Land-cover, topographic, and soil data were needed to generate the static physiographic database used by the model to define the watershed. Green Kenue is the software that was used to generate the physiographic database. The forcing data required by MESH include incoming shortwave radiation, incoming longwave radiation, temperature, wind speed, barometric pressure, precipitation, and specific humidity at a 30-min temporal resolution. All of these variables were measured at the OBS and OJP intensive observational sites. As such, the OBS forcing was used for the portion of the watershed in the Whiteswan Uplands, and the OJP forcing was used for the portion of the watershed in the White Gull Plains.

The forcing data had 1%–5% of values missing for all variables. Missing data were infilled using the nearby Boreal Ecosystem Research and Monitoring Sites (BERMS) flux towers, based on regression relationships. The regression relationships were estimated using moving windows of a few days to a few weeks and based on periods from the same time of day.

The land-cover data for the study area were derived from the Land Cover, circa 2000-Vector (LCC200-V) database (Natural Resources Canada 2015). LCC2000-V is the result of vectorization of raster thematic data originating from classified *Landsat 5* and *Landsat 7*

ortho images with the circular map accuracy standard (CMAS) of 30 m or better and is distributed as 1:250 000-scale National Topographic System (NTS) tiles. The land-cover map (Fig. 2d) and ecodistrict map (Fig. 2b) were clipped using the White Gull Creek basin boundary map (Fig. 2c). Clipped land-cover and ecodistrict maps were then dissolved so that the land-cover attributes could be recomputed for each ecodistrict. Land-cover data in each ecodistrict were regrouped into four of the land-cover types recognized by CLASS (needleleaf, broadleaf, grass, and bare soil), the percentages of which can be found in Table 3. The land cover classified as grasslands here is actually fens, which tend to have a water table near or above the peat surface.

The topographic data for the study area are obtained from the Canadian Digital Elevation Data (CDED) at the scale of 1:50 000 that are extracted from the hypsographic and hydrographic elements of the National Topographic Data Base (NTDB) or various scaled positional data acquired from the provinces and territories. For the 1:50 000 NTS tiles, depending on the latitude of the CDED section, the resolution varies from a minimum of 11 m to a maximum of 16 m in the east–west direction, while maintaining a resolution of 23 m in the north–south direction (Natural Resources Canada 2007).

Soil texture data were extracted from ecological framework attributed data produced by Agriculture and Agri-Food Canada. Percentage distribution of the parent material texture in each ecodistrict was compiled and made available for users at the Agriculture and Agri-Food Canada National Ecological Framework website (Agriculture and Agri-Food Canada 2015). Sand and clay fractions estimated from the soil texture classification triangle were used to establish parameter value ranges for calibration.

b. *Model setup*

MESH was set up as a semidistributed model with grid cells of about 15 km × 15 km (as shown in Fig. 2b). Subgrid variability was managed by using a combination of the GRU approach from Kouwen and Mousavi (2002) and the CLASS effective tile (Fig. 1a). The GRUs were set by ecodistrict and the effective tiles were configured by land cover for each ecodistrict.

1) MODEL RUN CONFIGURATIONS

The MESH model was run in four different configurations to compare two different parameter estimation techniques (a priori estimation vs calibration) and to explore limitations in how lateral flow is represented in MESH (see appendix A for details). The four configurations were:

TABLE 3. Percentage of land-cover classification of Whiteswan Uplands and White Gull Plains used in MESH.

Ecodistrict	NL (%)	BL (%)	*G* (%)	*B* (%)
Whiteswan Uplands	57.1	17.8	22.3	2.8
White Gull Plains	41.2	19.6	35.7	3.5

1) flat CLASS with a priori parameter values—using CLASS's representation of overland flow, no interflow, and predefined parameters;
2) flat CLASS with parameter calibration—using CLASS's representation of overland flow, no interflow, and automatically calibrated parameters;
3) sloped CLASS with a priori parameter—using MESH's representation of overland flow and interflow and predefined parameters; and
4) sloped CLASS with parameter calibration—using MESH's representation of overland flow and interflow and automatically calibrated parameters.

A priori parameter values and calibration parameter ranges (appendix B) were selected from the literature and technical documentation, or user defined when the literature values are nonexistent. The model was run from 1 October 1999 to 31 December 2014. Parameters were calibrated to fit daily streamflow observed at the White Gull Creek outlet. Calibration and validation periods were selected such that low- and high-flow years were present in the calibration period. An extremely high flow year is present in the validation period (2011). The period from 1 October 1999 to 31 December 2000 was used as a spinup period, 1 January 2001 to 31 December 2007 was used for the calibration period, and 1 January 2008 to 31 December 2014 was used for validation. Although calibration was performed only for streamflow, validation was performed on both streamflow and evapotranspiration, with some minimal analysis performed for soil moisture. Because of data availability for soil moisture and evapotranspiration, the validation on these two variables is limited to 2001–11 for soil moisture and 2001–09 for evapotranspiration.

2) CALIBRATION AND VALIDATION STATISTICS

A very simple multiobjective approach was used for calibrating the model. The Nash–Sutcliffe (NS) efficiency criteria (Nash and Sutcliffe 1970) of both the daily flows and the log of the daily flows were used for model calibration of streamflow, each with a 50% weighting. These two objective functions were selected because the NS values favor peak flows and the NS of the log of daily flows favors low flows, balancing MESH's ability to simulate both high and low flows. Based on the guidelines of Moriasi et al. (2007),

however, NS and percent bias (PBIAS) were used as verification of streamflow for all model configurations and separately for the calibration and validation periods. The calibration and validation periods were chosen using the split-sampling strategy as described by Klemeš (1986). Ostrich optimization and calibration software (Matott et al. 2009) with the dynamically dimensioned search (DDS) algorithm (Tolson and Shoemaker 2007) was used to fit simulated streamflow with observed streamflow with 1000 runs for each configuration that required calibration.

Box-and-whisker plots of evapotranspiration were also considered in the verification of the model for the calibration and validation periods for all model configurations. To compute evapotranspiration (ET; $\mathrm{mm\,s^{-1}}$) at the respective sites, latent heat flux (QE; $\mathrm{W\,m^{-2}}$) and temperature T (°C) observed at the two flux tower sites (OBS and OJP) were used in conjunction with the latent heat of vaporization λ ($\mathrm{J\,kg^{-1}}$) as follows:

$$\mathrm{ET} = \frac{\mathrm{QE}}{\lambda}, \tag{1}$$

where

$$\lambda = \begin{cases} 2501 - 2.37T & \text{for} \quad T \geq 0 \\ 2834 - 0.3039T - 0.0045T^2 & \text{for} \quad T < 0 \end{cases}. \tag{2}$$

The equations to calculate the latent heat of vaporization from temperature are derived from fitting regression equations to the values in Table 2.1 of Rogers and Yau (1989).

Latent heat flux is observed at the two flux towers using eddy covariance correlation. Eddy covariance has been known to systematically undermeasure sensible and latent heat flux (Falge et al. 2001; Hollinger and Richardson 2005; Moncrieff et al. 1997; Morgenstern et al. 2004). For example, Falge et al. (2001) found measured energy to be less on average by 13%. Based on 10 years of flux data measured at seven eddy covariance sites in and around White Gull Creek, Barr et al. (2012) found an energy closure factor of 0.85 to fit the White Gull basin. As a result, observed evapotranspiration at the flux tower sites is adjusted with this closure factor and the model output evapotranspiration compared against the adjusted evapotranspiration values at the 30-min interval. Gaps in the latent heat flux were filled using the Fluxnet-Canada standard method (Amiro et al. 2006).

c. Default parameters and ranges

Values and ranges for CLASS and hydrology model parameters for the a priori and calibration runs were determined based on readily available information or defined by the modeler when values and ranges were not readily available. Although more detailed information exists for a number of locations in this particular basin, this study is meant to replicate what is possible in parts of the world that have not been studied so intensely. The sources for parameter values include the CLASS technical documentation (Verseghy 2011), the National Ecological Framework for Canada (Agriculture and Agri-Food Canada 2015), and textbook values (e.g., Dingman 1994).

d. Results

The results of the four model configurations are presented first, comparing the model output with observations. The resulting discussion addresses the issues of parameter estimation, lateral hydrological processes, and subgrid heterogeneity.

1) STREAMFLOW

Figure 3 shows the NS and PBIAS results for each model configuration for the streamflow calibration and validation time periods as well as the corresponding hydrographs. The NS values gradually improve from Figs. 3a to 3d, although the bias values only improve with calibration. Despite the improved results when calibrating the flat configuration, this approach fails to capture most of the observed peak flows and overestimates most of the hydrograph recessions. The best results (in terms of NS) for both the calibration and validation time periods are the sloped configuration that was calibrated. The most obvious problem with the sloped, calibrated simulation is that the peaks tend to be overestimated in the dry years while being underestimated in the wet years. An obvious failure of all model configurations is in missing the very high peaks in the summer of 2011. Although it is possible that the observed streamflow is incorrect, we are fairly confident in both the streamflow measurement and the precipitation observations used to force MESH.

2) EVAPOTRANSPIRATION

Figure 4 shows box-and-whisker plots of the annual evapotranspiration values for the OBS and OJP flux towers and four model configurations for each grid cell where the flux towers are located. In all a priori model runs, the annual ET in the model is higher than the observations. When calibrated to streamflow, however, the annual ET box plots more closely align with the observations, particularly for the OBS site. There is still a discrepancy with the OJP site for the calibrated runs, which will be discussed in the subgrid heterogeneity section. Further analysis of ET (not shown) indicates that there is very little difference between the ET model output statistics for the streamflow calibration and validation time periods.

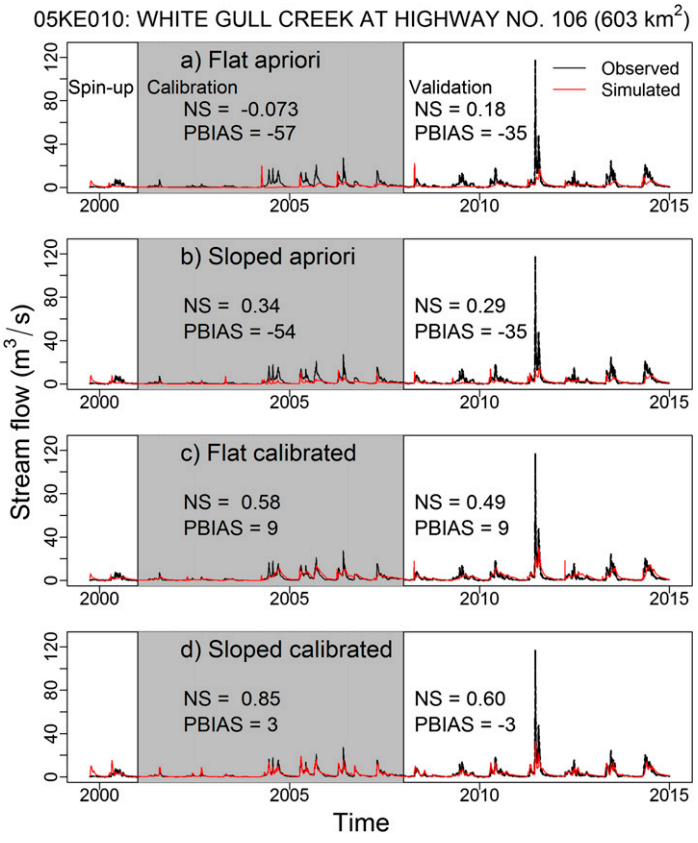

FIG. 3. Observed (black) and simulated (red) hydrographs for (a) flat a priori configuration, (b) sloped a priori configuration, (c) flat calibrated configuration, and (d) sloped calibrated configuration. The period from 1 Oct 1999 to 31 Dec 2000 is the spinup period; 1 Jan 2001 to 31 Dec 2007 is the calibration period; and 1 Jan 2008 to 31 Dec 2014 is the validation period. NS and PBIAS results are shown on the graph for each configuration for the calibration and validation periods. A positive bias indicates that the modeled average flow is higher than the observed average flow.

Figure 5 shows box-and-whisker plots of the daily OBS and OJP evapotranspiration values by month from 1 January 2001 to 30 September 2009. The most significant periods of ET occur from April to October. The November–March interquartile range is clearly higher for the observations, but the overall impact on cumulative ET results from differences between the observations and model output in the April–October period.

3) STORAGE

Although not studied in great detail here, observations of changes in water storage have been collected and analyzed for a number of locations in and around White Gull Creek [data extended to 2011 from Barr et al. (2012) and shown in greater detail]. To see if the model configurations generally capture the trends in soil moisture storage, Fig. 6 compares the measured change in storage with the four model configurations. The observed storage at the OBS and OJP sites do not always align with one another. For half of the water years from 2001 to 2011, the OBS and OJP sites show storage changes of opposite sign. Table 4 shows the annual mean and standard deviation for the period of record for both observations and the four model run configurations.

e. Discussion of results

The results of the case study are discussed with respect to the important issues raised earlier in the paper regarding parameter estimation, surface heterogeneity, and hydrologic process representation.

1) PARAMETER ESTIMATION

Calibration to streamflow clearly has an influence on the modeled latent heat fluxes to the atmosphere in this case study. Even with a relatively simple representation of subgrid heterogeneity and some obvious disconnects

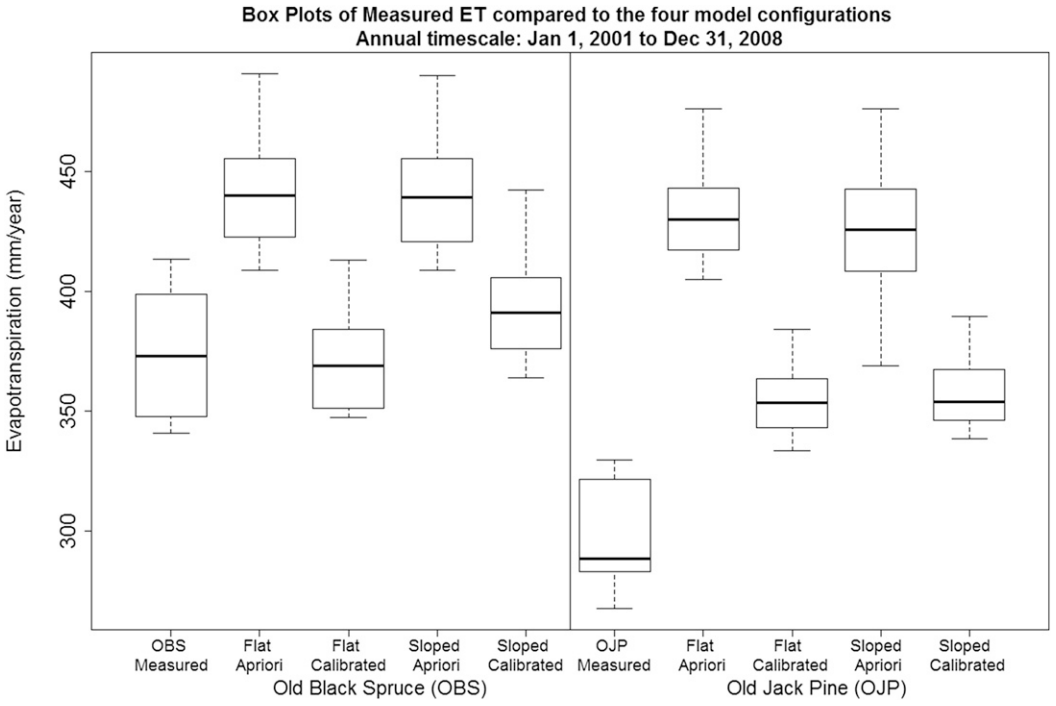

FIG. 4. Box plots of annual ET for OBS and OJP measurements and model outputs for 2001–08. The middle line in each box represents the median of the data, the bottom and top of the box are the 25th and 75th percentiles (respectively), and the ends of the whiskers extend to the data extremes.

between the real-world physical processes and how MESH represents those processes, calibrating the parameters made a significant difference in the model's ability to simulate ET. It is possible that the results would be different in other locations where alternative hydrological processes are dominant, but we suspect that these results would hold true elsewhere, and particularly for other relatively flat basins dominated by evapotranspiration. It is also possible that a priori estimates of parameter values in LSS applications could be made to be more appropriate than the selections made in this study. It is worth noting that ET bias is equally improved between calibrating flat or sloped CLASS to streamflow. A multiobjective calibration approach that includes the evaporative fluxes could be performed to explore this issue in greater detail.

As an alternative to calibrating to streamflow to determine parameters, Santanello et al. (2013) provide an example of calibrating 29 parameters to sensible, latent, and soil heat fluxes at 18 locations (with only six locations containing measurements of soil heat flux) using the Noah model. These calibrated parameters were then regionalized by generating new lookup tables for soil, vegetation, and general parameters across the study region, with promising results for both offline and coupled land–atmosphere model runs. In the spirit of Gupta et al. (1999), a multiobjective calibration approach could be applied using heat flux, soil moisture, and streamflow observations. Given the ubiquity of streamflow observations globally, the atmospheric modeling community has an opportunity to examine the value of streamflow (in addition to satellite-based observations of soil moisture) in helping estimate land surface parameter values to constrain their models for predicting atmospheric fluxes.

In terms of streamflow prediction, not surprisingly, calibration also has a positive influence on the modeled streamflow. Although some problems clearly remain, particularly for the flooding that occurred in June 2011. These problems will be discussed in the next sections [sections 6e(2) and 6e(3)].

2) SUBGRID HETEROGENEITY

The grid squares used for MESH (Fig. 2b) were much larger than the scales of the observations at the OBS and OJP field sites (Fig. 2c). In addition, a relatively simple representation of subgrid heterogeneity was employed in the model. These two choices make it somewhat challenging to compare the observations with the model output. It can be argued that the OBS site is representative of the hydrological processes over a larger area, but the same cannot necessarily be said for the OJP site (G. Van der Kamp 2015, personal communication). Because of the dry nature of the OJP site, it is possible

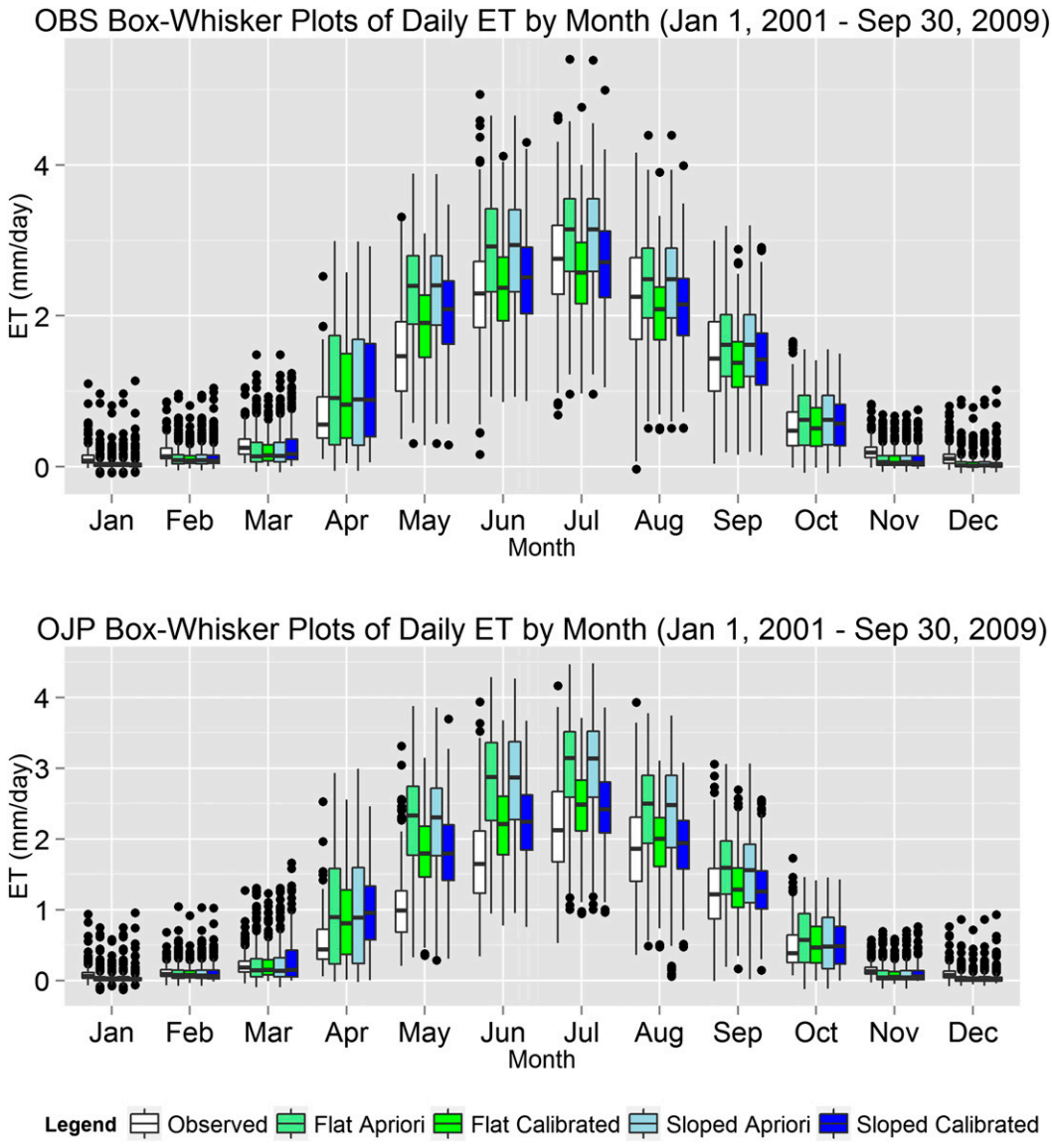

FIG. 5. Box plots of daily ET for (top) OBS and (bottom) OJP measurements and model outputs on a monthly basis from 1 Jan 2001 to 30 Sep 2009. The upper whisker extends from the hinge to the highest value, that is, within 1.5 times the interquartile range of the hinge, where the interquartile range is the distance between the first and third quartiles. Data beyond the end of the whiskers are considered outliers and are plotted as points.

that the model results for the grid cell encompassing the OJP site are representative of the grid cell average ET because much of the grid cell would generally be wetter than the location of the measurements. As such, the point observations of ET would be lower than the grid cell average ET, as is the case shown in Fig. 4.

Further study is needed to examine the impact of smaller grid cells and other configurations of representing surface heterogeneity on the ability of MESH to model the various components of the water balance. Either scaling up the observations or scaling down the model output would help in comparing the two. One obvious place to look for answers to the model's ability to simulate ET at short time scales is to do a more detailed comparison of the observed storage terms to those of the model, although spatial scaling issues will still need to be considered for any accurate analysis.

We suspect that the failure of the model to predict the June 2011 flooding is because of how surface heterogeneity is represented in this model setup. The effective tile of CLASS within each ecodistrict GRU does not accurately represent the wetland areas in the basin.

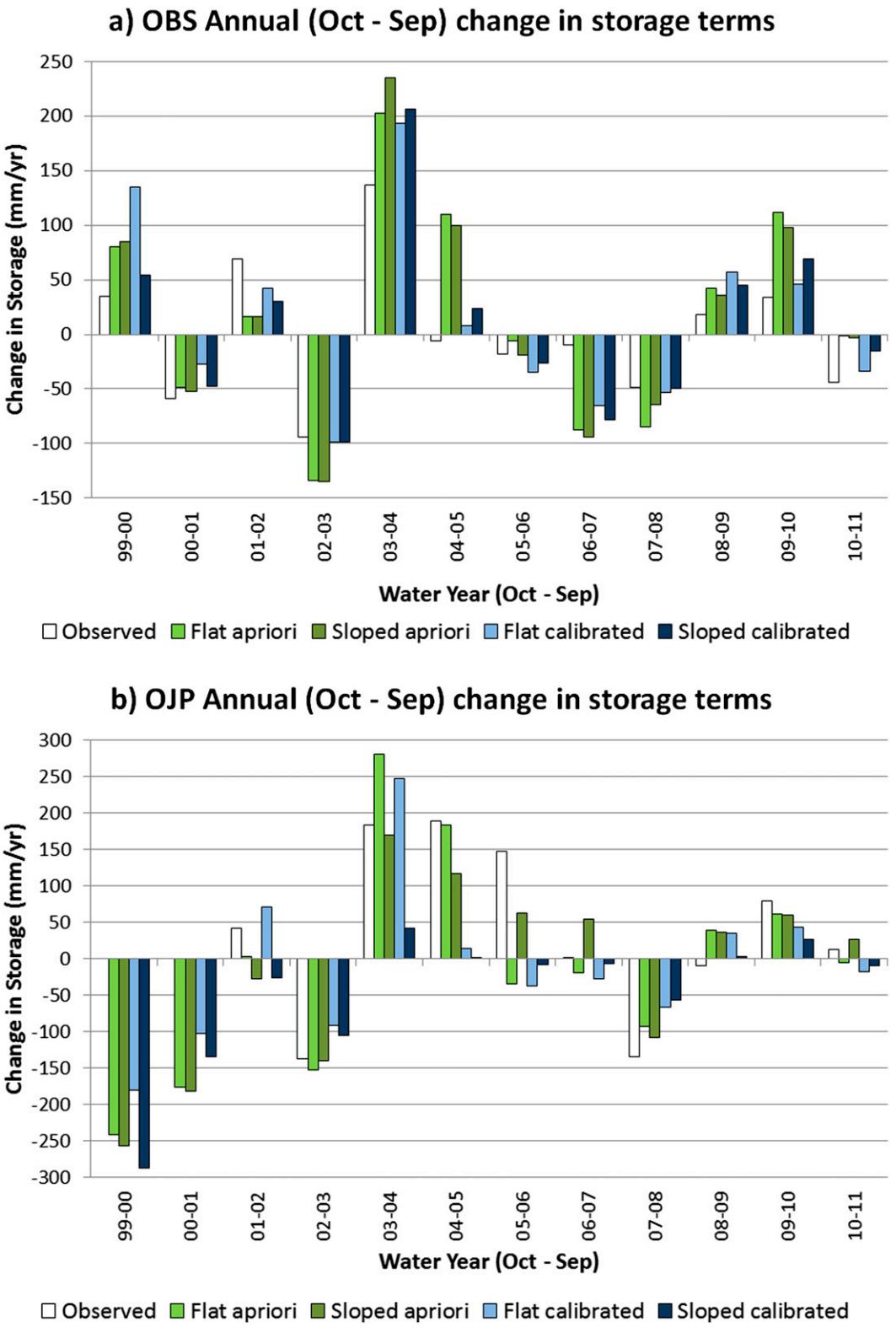

FIG. 6. Annual changes in storage at (top) OBS and (bottom) OJP (measured and modeled) from 1 Oct 1999 to 30 Sep 2011.

TABLE 4. Annual mean (std dev in parentheses) of the observed and modeled ΔS (mm yr^{-1}) for OBS and OJP. The period is for hydrological years from 1 Oct 1999 to 30 Sep 2011 for OBS and from 1 Oct 2001 to 30 Sep 2011 for OJP.

Configuration	OBS	OJP
Observed	1 (63)	38 (116)
Flat a priori	17 (98)	26 (127)
Flat calibrated	14 (86)	17 (95)
Sloped a priori	17 (102)	25 (95)
Sloped calibrated	9 (82)	−14 (42)

Although a wetland algorithm does not currently exist in MESH, we postulate that the wetlands can be characterized and parameterized in terms of vegetation, soil, and land surface parameters to better simulate both the peak- and low-flow periods, especially for the June 2011 flooding event, as will be discussed next.

3) HYDROLOGICAL PROCESSES IN WHITE GULL CREEK

We speculate that the flooding in 2011 is the result of saturation excess overland flow from wetlands within the basin, which was not captured by the model at all. In fact, the modeled flow for this event was almost entirely from interflow. The rainfall leading up to the June 2011 flooding was on the order of 100 mm over several days. These rains caused the water level in the fen site shown in Fig. 2c to rise 200 mm and then drain about 103 mm before the next big rainfall event in mid-July, which added another 100 mm of water to the wetland. Throughout the entire period of May–December 2011, water levels in the fen were above the ground surface, peaking on 21 June at 300 mm above the peat surface (R. Schmidt 2016, personal communication). We suspect that the heavy June and July rains pushed the water levels past a threshold that allowed the many wetland areas in the basin to move relatively large amounts of water to the stream network, causing the two peaks seen in the observed flow in June and July 2011. Because of the representation of subgrid heterogeneity in the model configuration, which did not account for the wetland soil and ponding characteristics in particular, it is unlikely that this particular setup of MESH would be able to predict this event.

At longer time scales, White Gull Creek is a basin dominated by evapotranspiration. As a result, latent heat fluxes to the atmosphere are sensitive to changes in lateral flow through the landscape and in the river channels. Subsurface flow and wetlands present two important controls to the amount and timing of water flowing to the stream. The water table varies considerably throughout the basin. The OBS site is located in an area with a water table that is near the surface most of the time, with lateral flow declining rapidly as the water table declines. The result is that wet areas of the basin, like the OBS site, generally maintain water for evapotranspiration while letting relatively little move laterally to the streams. The OJP site is located in a very dry part of the basin with a water table that ranges from 5 to 7 m below the surface. This extremely dry location of the basin releases relatively little water to the atmosphere by evapotranspiration but is able to maintain a steady flow of water to the stream via groundwater. At a nearby wetland fen site, assumed to characterize other wetlands that are a significant percentage of the basin, the water table ranges from below the surface to above the surface, storing water in wet years and gradually releasing water in dry years (Barr et al. 2012). As already discussed, the exception to this rule may be when the water levels in the wetlands pass some threshold that then cause water to move quickly to the stream network.

It appears that MESH is usually able to mimic the sign of the storage and release of water over large areas at the annual time scale, as shown in Fig. 6. Exceptions include the water year 2004/05 for OBS and a number of the configurations for some years for OJP. Because of the difference in scale between the observations and the model output, it is difficult to make any conclusions based on the results in Fig. 6 and Table 4. Other configurations of the model, such as using smaller grid cells or different GRUs, could help in making this comparison more meaningful.

The relatively comparable ET results for the calibrated runs at the OBS site may be due to how the MESH soil layers were configured. The model was set up to have three soil layers of 10 cm, 25 cm, and 3.75 m thickness, respectively. With calibration, both the CLASS and MESH representations of subsurface flow may have allowed for the right amount of soil moisture to be available for ET. It would be interesting in future studies, however, to make use of the CLASS wetland soil properties controlling vertical water fluxes. Because of the fact that the OJP site is located in a very dry part of the basin, the ET results are more difficult to interpret, as already discussed in the section on subgrid heterogeneity.

7. Conclusions

The question remains as to what is missing from the prescription of hydrology for land surface schemes. Throughout this paper, we have explored three ideas that we feel could further benefit the land surface modeling community and make LSSs more appealing for the hydrologic modeling community: 1) improvements to the incorporation of lateral hydrologic

TABLE B1. Fixed land-cover parameters used in all four configurations of MESH.

Parameter name	Description	Units	NL	BL	*G*	Source
QA50	Reference value of incoming shortwave radiation used in stomatal resistance formula	$W\,m^{-2}$	30	40	30	Verseghy (2011)
VPDA	Vapor pressure deficit coefficient used in stomatal resistance formula	—	0.65	0.5	0.5	Verseghy (2011)
VPDB	Vapor pressure deficit coefficient used in stomatal resistance formula	—	1.05	0.6	1.0	Verseghy (2011)
PSGA	Soil moisture suction coefficient used in stomatal resistance formula	—	100	100	100	Verseghy (2011)
PSGB	Soil moisture suction coefficient used in stomatal resistance formula	—	5	5	5	

processes, 2) more flexible methods to represent surface heterogeneity, and 3) better use of existing parameter estimation techniques and streamflow observations.

As Table 2 illustrates, many LSSs have begun the process of incorporating lateral hydrologic processes into their modeling toolkits. The focus has generally been on overland flow, groundwater, and river routing, with only a few LSSs considering other important lateral hydrologic processes. As such, we encourage the continued progression of incorporating lateral process algorithms into LSSs, which appears to be in the early stages of development. In addition, as Clark et al. (2015a) highlight, there are many options to consider when looking to incorporate various hydrologic processes in LSSs. These options should be systematically explored as H-LSSs develop.

In terms of spatial heterogeneity in LSSs, this is an area that requires much more exploration as it seems underexamined in the scientific literature, despite the fact that every land surface modeler needs to deal with the issue. This paper does not provide any guidance on how spatial heterogeneity should be incorporated into modeling efforts, but rather focuses on identifying key aspects of the decisions that a modeler must make. The case study also highlights the challenges associated with comparing observations taken at one scale with model output at another scale. The results of the case study indicate that the choices taken to represent spatial heterogeneity in the basin are not appropriate for the 2011 flood event that occurred.

One method of dealing with spatial heterogeneity is the hyperresolution modeling activities of Wood et al. (2011). These efforts are certainly laudable and should be explored, but the trade-offs in terms of model complexity versus model efficiency may not be worth it for some applications. It is also unclear if the increase in model complexity will necessarily result in improvements to model fidelity. In this regard, the efforts of Clark et al. (2015b) for examining various modeling alternatives is very much needed to shed light on the issues surrounding complexity, efficiency, and fidelity.

Parameter estimation techniques have come a long way from expert, manual calibration of hydrologic models in the 1960s. The case study illustrates that model calibration shows potential when compared to a priori parameter estimation. If weather and climate models continue to use a priori parameter values for land surface parameterization, then these values need some very careful consideration. For ensemble modeling applications, these results show that land surface parameter perturbation is a worthwhile endeavor to produce ensemble members, although choosing the appropriate members of a parametric ensemble with the large parameter spaces of LSSs is hardly trivial.

The study does not explore the many issues surrounding various sources of uncertainty in any modeling exercise, and this will be important to consider in future work. However, the availability of streamflow as an integrated watershed response provides a unique opportunity (among other opportunities) for atmospheric modelers to improve upon the current practice of using lookup tables to define parameter values.

As a final note, similar case studies should be performed at more locations and with a greater variety of model configurations, making use of the benchmarking ideas described by Clark et al. (2015a).

Acknowledgments. We gratefully acknowledge Environment and Climate Change Canada and Hydro-Québec for funding this study. We also gratefully acknowledge Fluxnet-Canada investigators Andy Black, Harry McCaughey, and Alan Barr for the flux-tower measurements at OBS and OJP and the Water Survey of Canada for the streamflow measurements. We would also like to thank the following colleagues for their insights in discussing the work: Garth van der Kamp, Alan Barr, Randy Schmidt, Paul Bartlett, and Diana Verseghy from Environment and Climate Change Canada; Andrew Ireson, Muluneh Mekonnen, and John Pomeroy from the University of Saskatchewan; and Ethan Johnson from Environment and Climate Change Canada for some much needed editorial assistance. Finally, we thank Martyn

TABLE B2. Fixed basinwide parameters used in all four configurations of MESH.

Parameter name	Description	Units	Basinwide parameter value	Source
DRN	Soil drainage index, set to 1 to allow the soil physics to determine drainage, and a value between 0 and 1 to simulate impeded drainage	—	1	Verseghy (2011)
SDEP	Soil permeable depth, set to greater than model soil depth to simulate fully permeable soil	m	8	Verseghy (2011)

Clark and two anonymous reviewers for their very helpful comments.

APPENDIX A

Process Representations in MESH (Using CLASS), ISBA, and SVS

For 11 LSMs, Clark et al. (2015a, their appendix A) clearly describe the storage and transmission of water through soils, root water uptake, groundwater dynamics, stream–aquifer–land interactions, and channel/floodplain routing. Of the LSMs described, seven are the same as the nine LSMs explored in this paper. As a result, the two remaining LSMs (ISBA and MESH) are described in a parallel manner to the description provided by Clark et al. (2015a). Since ISBA is in the process of being replaced by SVS at Environment and Climate Change Canada (Alavi et al. 2016; Husain et al. 2016), major improvements to ISBA that have been implemented in SVS are also discussed. It should also be mentioned that the version of ISBA used in Canada for numerical weather prediction is different from the operational version used by Météo-France. The Canadian version of ISBA is described in detail by Bélair et al. (2003a,b). The description of ISBA in this appendix is also for the Canadian version of ISBA.

a. Storage and transmission through soils

Clark et al. (2015a) note that most LSMs, including MESH, SVS, and ISBA, use the one-dimensional Richards' equation to simulate the storage and transmission of water through soils, as shown in Eq. (A1):

$$\frac{\delta\theta}{\delta t} = -\frac{\delta q}{\delta z} + S_{\mathrm{ET}} + S_{\mathrm{lf}}, \tag{A1}$$

where θ is the volumetric liquid water content, t is time (s), q is the vertical flux of liquid water (m s^{-1}), z is depth (m), S_{ET} is the sink term for evapotranspiration (root water uptake), and S_{lf} is the source–sink term for the lateral flux of liquid water (s^{-1}). The vertical flux of water leads to the moisture-based form of Richard's equation:

$$q(z) = -K\frac{d\psi}{d\theta}\frac{\delta\theta}{\delta z} + K, \tag{A2}$$

where $K = f(\theta)$ is the hydraulic conductivity (m s^{-1}) and $\psi = f(\theta)$ is the liquid water matric potential (m).

Differences between the LSMs are mainly due to differences in how Eqs. (A1) and (A2) are implemented. Within MESH, most of the soil moisture storage and transport processes (including the upper- and lower-boundary conditions) are managed by CLASS. Exceptions include the upper-boundary conditions as represented by the partitioning of surface runoff as well as the lateral flux term (i.e., S_{lf}) in Eq. (A1), which are included in MESH, but not CLASS.

In terms of the lateral flux term, CLASS is similar to many other LSMs by setting this term to zero. MESH improves upon CLASS's representation of subsurface lateral flow by calculating both saturated and unsaturated lateral flow. This is accomplished using a parameterization that computes lateral flow from the bulk

TABLE B3. Fixed basinwide parameters used in sloped configurations of MESH.

Parameter name	Description	Units	Basinwide parameter value	Source
DDEN	Drainage density, equal to the length of the stream divided by area drained by the stream	km km^{-2}	50	Dingman (2002)
XSLP	Average overland slope	Rise/run	0.01	User defined
GRKF	Ratio of saturated horizontal hydraulic conductivity at a depth of 1 m to the saturated horizontal hydraulic conductivity at the surface	—	0.01	User defined

TABLE B4. A priori parameters, parameter ranges, and calibrated parameters in the four configurations of MESH.

Parameter name	Description	Units	A priori	Lower limit	Upper limit	Flat calibrated	Sloped calibrated	Source
LANZ0-NL	Natural log of roughness length (needleleaf)	ln(m)	0.405	0	0.69	0.316	0.654	Verseghy (2011)
LANZ0-BL	Natural log of roughness length (broadleaf)	ln(m)	0.69	0	1.1	0.266	1.061	Verseghy (2011)
LANZ0-GR	Natural log of roughness length (grass)	ln(m)	−2.526	−3.912	−1.966	−2.917	−1.972	Verseghy (2011)
ALVC-NL	Visible albedo (needleleaf)	—	0.03	0.02	0.1	0.047	0.092	Verseghy (2011)
ALVC-BL	Visible albedo (broadleaf)	—	0.05	0.02	0.1	0.054	0.049	Verseghy (2011)
ALVC-GR	Visible albedo (grass)	—	0.05	0.02	0.1	0.057	0.071	Verseghy (2011)
ALIC-NL	Near-infrared albedo (needleleaf)	—	0.19	0.1	0.3	0.252	0.257	Verseghy (2011)
ALIC-BL	Near-infrared albedo (broadleaf)	—	0.29	0.2	0.4	0.391	0.26	Verseghy (2011)
ALIC-GR	Near-infrared albedo (grass)	—	0.31	0.2	0.4	0.293	0.381	Verseghy (2011)
RSMN-NL	Min stomatal resistance (needleleaf)	$s\,m^{-1}$	200	150	250	239.8	218.221	Verseghy (2011)
RSMN-BL	Min stomatal resistance (broadleaf)	$s\,m^{-1}$	125	75	175	172.1	127.806	Verseghy (2011)
RSMN-GR	Min stomatal resistance (grass)	$s\,m^{-1}$	100	50	150	138.3	145.318	Verseghy (2011)
LAMAX-NL	Max leaf area index (needleleaf)	—	2	1.8	3	1.9278	1.8646	Verseghy (2011)
LAMAX-BL	Max leaf area index (broadleaf)	—	6	3	10	4.0277	3.1602	Verseghy (2011)
LAMAX-GR	Max leaf area index (grass)	—	4	4	6	4.9826	4.368	Verseghy (2011)
LAMIN-NL	Min leaf area index (needleleaf)	—	1.6	0.5	1.8	0.8106	0.804	Verseghy (2011)
LAMIN-BL	Min leaf area index (broadleaf)	—	0.5	0.1	3	1.1202	2.759	Verseghy (2011)
LAMIN-GR	Min leaf area index (grass)	—	4	0	4	3.0086	1.6915	Verseghy (2011)
MAXMASS-NL	Standing biomass density (needleleaf)	$kg\,m^{-2}$	25	10	40	39.174	39.845	Verseghy (2011)
MAXMASS-BL	Standing biomass density (broadleaf)	$kg\,m^{-2}$	20	5	35	34.369	24.152	Verseghy (2011)
MAXMASS-GR	Standing biomass density (grass)	$kg\,m^{-2}$	3	1	5	4.83	3.293	Verseghy (2011)
ROOT-NL	Root depth (needleleaf)	m	1	0.05	3	0.95404	0.60514	Verseghy (2011)
ROOT-BL	Root depth (broadleaf)	m	2	0.05	3	2.84804	0.642	Verseghy (2011)
ROOT-GR	Root depth (grass)	m	1.2	0.05	3	1.87154	1.15928	Verseghy (2011)
MANN-WSU	Manning's n for overland flow (Whiteswan Uplands)	$m\,s^{-1/3}$	0.05	0.01	0.16	—	0.087	Dingman (2002)
MANN-WGP	Manning's n for overland flow (White gull Plains)	$m\,s^{-1/3}$	0.05	0.01	0.16	—	0.015	Dingman (2002)
KS-WSU	Saturated surface horizontal soil conductivity (Whiteswan Uplands)	$m\,s^{-1}$	0.001	0.00001	0.1	—	0.00084	User specified
KS-WGP	Saturated surface horizontal soil conductivity (White gull Plains)	$m\,s^{-1}$	0.001	0.00001	0.1	—	0.05084	User specified
SAND-L1-WSU	Sand in soil layer 1 (Whiteswan Uplands)	%	61	50	80	79.5	72.6	Ecodistrict based
SAND-L2-WSU	Sand in soil layer 2 (Whiteswan Uplands)	%	61	50	80	80	50.6	Ecodistrict based
SAND-L3-WSU	Sand in soil layer 3 (Whiteswan Uplands)	%	61	50	80	79.8	61.5	Ecodistrict based
CLAY-L1-WSU	Clay in soil layer 1 (Whiteswan Uplands)	%	12	5	20	13.3	10.4	Ecodistrict based
CLAY-L2-WSU	Clay in soil layer 2 (Whiteswan Uplands)	%	12	5	20	5	17.2	Ecodistrict based
CLAY-L3-WSU	Clay in soil layer 3 (Whiteswan Uplands)	%	12	5	20	14.6	5.9	Ecodistrict based
SAND-L1-WGP	Sand in soil layer 1 (White Gull Plains)	%	87	80	90	85.8	86.1	Ecodistrict based

TABLE B4. (*Continued*)

Parameter name	Description	Units	A priori	Lower limit	Upper limit	Flat calibrated	Sloped calibrated	Source
SAND-L2-WGP	Sand in soil layer 2 (White Gull Plains)	%	87	80	90	89.9	88.8	Ecodistrict based
SAND-L3-WGP	Sand in soil layer 3 (White Gull Plains)	%	87	80	90	88.4	89.6	Ecodistrict based
CLAY-L1-WGP	Clay in soil layer 1 (White Gull Plains)	%	8	5	10	8.9	7.1	Ecodistrict based
CLAY-L2-WGP	Clay in soil layer 2 (White Gull Plains)	%	8	5	10	5.4	8.1	Ecodistrict based
CLAY-L3-WGP	Clay in soil layer 3 (White Gull Plains)	%	8	5	10	9.9	7.7	Ecodistrict based
ZSNL-WSU	Limiting snow depth below which coverage is <100% (Whiteswan Uplands)	m	0.1	0.03	1	0.16	0.15	User specified
ZSNL-WGP	Limiting snow depth below which coverage is <100% (White Gull Plains)	m	0.1	0.03	1	0.2	1	User specified
ZPLS-WSU	Max water ponding depth for snow-covered areas (Whiteswan Uplands)	m	0.1	0.005	0.5	0.12	0.29	User specified
ZPLS-WGP	Max water ponding depth for snow-covered areas (White Gull Plains)	m	0.1	0.005	0.5	0.09	0.42	User specified
ZPLG-WSU	Max water ponding depth for snow-free areas (Whiteswan Uplands)	m	0.1	0.005	0.5	0.12	0.38	User specified
ZPLG-WGP	Max water ponding depth for snow-free areas (White Gull Plains)	m	0.1	0.005	0.5	0.02	0.3	User specified
WF-R2	River roughness factor combining channel shape, width to depth ratio, and Manning's n	$m^{1/2}\,s^{-1}$	1	0.3	3	0.303	1.459	User specified

value of soil moisture in the soil layer, by means of an approximation of Richard's equation (Soulis et al. 2000, 2011). Vertical redistribution of water and lateral fluxes of liquid water are computed in the same manner in SVS. The Canadian version of ISBA relies instead on a much simpler force-restore parameterization.

1) INFILTRATION AND SURFACE RUNOFF

The upper-boundary condition of Eq. (A1) is the surface infiltration and is described in Clark et al. (2015a) as

$$q(z=0) = P_X - e_s - q_s, \tag{A3}$$

where P_X is the soil surface flux from rainfall, throughfall, canopy drip, and drainage from the bottom of the snowpack; e_s is bare soil evaporation; and q_s is surface runoff (all units in $kg\,m^2\,s^{-1}$). In the LSMs considered, a wide variety of approaches have been used to represent surface runoff in particular.

Overland flow in CLASS is limited to excess water above a ponding depth on the surface. The pond is filled by both saturation excess and infiltration excess of the soil. As such, CLASS inherently includes a threshold-based mechanism for both saturation excess and infiltration excess overland flow. The model does not, however, have any representation of overland flow routing to a stream network or interconnectivity of surface storage potential. SVS and ISBA use a similar mechanism for generating surface runoff, but do not include ponded water as a prognostic variable. Hence, any saturation or infiltration excess occurring on a given model time step is immediately removed from the land surface scheme and sent to the river network.

MESH improves upon CLASS's representation of overland flow in a number of ways (Soulis et al. 2000; Soulis and Seglenieks 2008; Mekonnen et al. 2014). First, the model uses Manning's equation for overland flow to route, from the land surface to a microdrainage network in a model grid cell, the water provided by ponds that overtop in CLASS (Soulis et al. 2000).

For areas such as the North American prairies where surface storage thresholds (e.g., in the form of

depressions on the landscape) control the amount of water available for overland flow, Mekonnen et al. (2014) showed that the probability distribution model (PDM) concept could replace the default CLASS ponding depths to simulate a subgrid distribution of surface depressions for more accurately predicting variable contributing areas for the calculation of overland flow. PDM-based runoff (ROF) generation (PDMROF) was implemented as a switch in MESH to replace the previously described overland and subsurface lateral flow algorithm. An interesting next step with PDMROF would be to use it to replace the CLASS ponding depths and to calculate the available water as an input to Manning's equation for overland flow, and still maintain MESH's interflow algorithm. This would preserve the interflow component while allowing for variable contributing areas.

2) THE BOTTOM BOUNDARY CONDITION FOR SOIL HYDROLOGY

The lower-boundary condition of Eq. (A1) is the surface infiltration and is described in Clark et al. (2015a) as

$$q(z = z_u) = \begin{cases} c_d K_i & \text{flux-boundary condition} \\ -K_{\text{sat}} \dfrac{-\psi(\theta_i)}{z_u - z_i} + K_{\text{sat}} & \text{head-boundary condition} \end{cases}, \tag{A4}$$

where z_u is the depth of the unsaturated zone (m), which is the depth of the water table for the head boundary condition; z_i is the depth of the lowest soil layer (m); K_i is the hydraulic conductivity of the lowest soil layer ($\mathrm{m\,s^{-1}}$); K_{sat} is the saturated hydraulic conductivity ($\mathrm{m\,s^{-1}}$); θ_i is the volumetric liquid water content of the lowest soil layer; and c_d is a parameter that controls the rate of flow at the lower boundary.

CLASS and MESH use the flux-boundary condition of Eq. (A4) with c_d as a parameter that can be set (or optimized) by the model user. ISBA and SVS use the head-boundary condition when bulk water content of the soil column is above field capacity, and a no-flux condition otherwise.

b. *Root water uptake*

Root water uptake in MESH is the same as CLASS and is a slight variation of the approach described in appendix A2 of Clark et al. (2015a). CLASS calculates the soil water suction (not volumetric water content) in each layer and then calculates the stress function based on the root-containing layer with the smallest soil water suction. The fraction of the total transpiration taken out of each soil layer in the rooting zone is calculated in a two-stage process. The fractional amount of root mass is calculated in each layer and then weighted by the relative soil moisture suction in the layer.

Root water uptake in SVS and ISBA is prescribed as a function of the rooting depth and the transpiration flux. ISBA relies on the Jarvis parameterization to estimate evapotranspiration, whereas SVS can use either the Jarvis model or a photosynthesis model (Husain et al. 2016).

c. *Groundwater dynamics*

The groundwater dynamics in MESH is represented by a combination of two of the approaches described by Clark et al. (2015a). The water that percolates from the bottom of the soil profile is called base flow in MESH, although this does not represent an explicit representation of groundwater dynamics. If the groundwater table is located within the soil column, however, S_{lf} in Eq. (A1) is the approach used by MESH. In this case, however, it is difficult to distinguish between unsaturated and saturated lateral flow in MESH. MESH calls the lateral flow from the soil column interflow, even though it can be a combination of interflow and base flow, while still referring to base flow when accounting for the water that percolates from the bottom of the soil profile.

The lateral flow is calculated using an approximation of Richard's equation that accounts for the bulk value of soil moisture (bulk saturation) within a CLASS soil layer (Soulis et al. 2000, 2011). Given the value of bulk saturation at the beginning of a time step, and assuming that this bulk saturation is the result of Darcian flow in the direction of the hillslope starting from a saturated soil (with no rain after than), there is a one-to-one relationship between bulk saturation and the time elapsed since the rain stopped. Knowing the initial bulk saturation, this allows for the calculation of the (theoretical) time elapsed since the soil was saturated. Adding the model time step then allows for the bulk saturation at the end of the time step to be calculated. The difference in bulk saturation from the beginning to the end of the time step is considered to be the interflow and includes both saturated and unsaturated lateral flow.

SVS uses the same approach as MESH for dealing with groundwater, whereas this process is absent from ISBA.

d. Stream–aquifer–land interactions

MESH, SVS, and ISBA do not explicitly represent stream–aquifer–land interactions. Any base flow generated by these models is assumed to contribute to streamflow.

e. Channel/floodplain routing

The routing in MESH, SVS, and ISBA is the same as the routing in WATFLOOD (Kouwen and Mousavi 2002), which is a simple kinematic wave method based on the continuity equation and Manning's formula.

APPENDIX B

Parameter Values and Ranges for the Four Model Configurations

A priori parameter values and calibration parameter ranges (Tables B1–B4) were selected from the literature and technical documentation, or user defined when the literature values were nonexistent.

REFERENCES

Agriculture and Agri-Food Canada, 2015: National ecological framework. Accessed 10 June 2016. [Available online at http://sis.agr.gc.ca/cansis/nsdb/ecostrat/index.html.]

Alavi, N., S. Bélair, V. Fortin, S. Zhang, S. Husain, M. Carrera, and M. Abrahamowicz, 2016: Warm season evaluation of soil moisture prediction in the Soil, Vegetation and Snow (SVS) scheme. *J. Hydrometeor.*, doi:10.1175/JHM-D-15-0189.1, in press.

Amiro, B., and Coauthors, 2006: Carbon, energy and water fluxes at mature and disturbed forest sites, Saskatchewan, Canada. *Agric. For. Meteor.*, **136**, 237–251, doi:10.1016/j.agrformet.2004.11.012.

Archfield, S. A., and Coauthors, 2015: Accelerating advances in continental domain hydrologic modeling. *Water Resour. Res.*, **51**, 10 078–10 091, doi:10.1002/2015WR017498.

Balsamo, G., A. Beljaars, K. Scipal, P. Viterbo, B. van den Hurk, M. Hirschi, and A. K. Betts, 2009: A revised hydrology for the ECMWF model: Verification from field site to terrestrial water storage and impact in the Integrated Forecast System. *J. Hydrometeor.*, **10**, 623–643, doi:10.1175/2008JHM1068.1.

Barr, A., G. Van der Kamp, T. Black, J. McCaughey, and Z. Nesic, 2012: Energy balance closure at the BERMS flux towers in relation to the water balance of the White Gull Creek watershed 1999–2009. *Agric. For. Meteor.*, **153**, 3–13, doi:10.1016/j.agrformet.2011.05.017.

Bastidas, L., T. S. Hogue, S. Sorooshian, H. Gupta, and W. Shuttleworth, 2006: Parameter sensitivity analysis for different complexity land surface models using multicriteria methods. *J. Geophys. Res.*, **111**, D20101, doi:10.1029/2005JD006377.

Becker, A., 1992: Criteria for a hydrologically sound structuring of large scale land surface process models. *Advances in Theoretical Hydrology*, Elsevier, 97–112.

Bélair, S., L.-P. Crevier, J. Mailhot, B. Bilodeau, and Y. Delage, 2003a: Operational implementation of the ISBA land surface scheme in the Canadian regional weather forecast model. Part I: Warm season results. *J. Hydrometeor.*, **4**, 352–370, doi:10.1175/1525-7541(2003)4<352:OIOTIL>2.0.CO;2.

——, R. Brown, J. Mailhot, B. Bilodeau, and L.-P. Crevier, 2003b: Operational implementation of the ISBA land surface scheme in the Canadian regional weather forecast model. Part II: Cold season results. *J. Hydrometeor.*, **4**, 371–386, doi:10.1175/1525-7541(2003)4<371:OIOTIL>2.0.CO;2.

Beltaos, S., 2008: Progress in the study and management of river ice jams. *Cold Reg. Sci. Technol.*, **51**, 2–19, doi:10.1016/j.coldregions.2007.09.001.

Best, M., and Coauthors, 2011: The Joint UK Land Environment Simulator (JULES), model description—Part 1: Energy and water fluxes. *Geosci. Model Dev.*, **4**, 677–699, doi:10.5194/gmd-4-677-2011.

Beven, K. J., 1996: A discussion of distributed hydrological modelling. *Distributed Hydrological Modelling*, M. B. Abbott and J. C. Refsgaard, Eds., Water Science and Technology Library, Vol. 22, Springer, 255–278, doi:10.1007/978-94-009-0257-2_13.

——, and H. L. Cloke, 2012: Comment on "Hyperresolution global land surface modeling: Meeting a grand challenge for monitoring Earth's terrestrial water" by Eric F. Wood et al. *Water Resour. Res.*, **48**, W01801, doi:10.1029/2011WR010982.

Bierkens, M. F., and Coauthors, 2015: Hyper-resolution global hydrological modelling: What is next? *Hydrol. Processes*, **29**, 310–320, doi:10.1002/hyp.10391.

Boone, A., and Coauthors, 2004: The Rhône-Aggregation Land Surface Scheme Intercomparison Project: An overview. *J. Climate*, **17**, 187–208, doi:10.1175/1520-0442(2004)017<0187:TRLSSI>2.0.CO;2.

Bowling, L. C., and D. P. Lettenmaier, 2010: Modeling the effects of lakes and wetlands on the water balance of arctic environments. *J. Hydrometeor.*, **11**, 276–295, doi:10.1175/2009JHM1084.1.

——, J. Pomeroy, and D. Lettenmaier, 2004: Parameterization of blowing-snow sublimation in a macroscale hydrology model. *J. Hydrometeor.*, **5**, 745–762, doi:10.1175/1525-7541(2004)005<0745:POBSIA>2.0.CO;2.

Branfireun, B. A., and N. T. Roulet, 1998: The baseflow and storm flow hydrology of a precambrian shield headwater peatland. *Hydrol. Processes*, **12**, 57–72, doi:10.1002/(SICI)1099-1085(199801)12:1<57::AID-HYP560>3.0.CO;2-U.

Chow, V. T., 1959: *Open Channel Hydraulics*. McGraw-Hill, 680 pp.

Clark, M. P., and Coauthors, 2015a: Improving the representation of hydrologic processes in Earth system models. *Water Resour. Res.*, **51**, 5929–5956, doi:10.1002/2015WR017096.

——, and Coauthors, 2015b: A unified approach for process-based hydrologic modeling: 1. Modeling concept. *Water Resour. Res.*, **51**, 2498–2514, doi:10.1002/2015WR017198.

Decharme, B., R. Alkama, F. Papa, S. Faroux, H. Douville, and C. Prigent, 2012: Global off-line evaluation of the ISBA-TRIP flood model. *Climate Dyn.*, **38**, 1389–1412, doi:10.1007/s00382-011-1054-9.

Dingman, S. L., 1994: *Physical Hydrology*. Prentice-Hall Inc., 575 pp.

——, 2002: *Physical Hydrology*. 2nd ed. Prentice-Hall Inc., 646 pp.

Duan, Q., and Coauthors, 2006: Model Parameter Estimation Experiment (MOPEX): An overview of science strategy and major results from the second and third workshops. *J. Hydrol.*, **320**, 3–17, doi:10.1016/j.jhydrol.2005.07.031.

Dunne, T., 1978: Field studies of hillslope flow processes. *Hillslope Hydrology*, M. J. Kirkby, Ed., Wiley, 227–293.

——, and R. D. Black, 1970a: An experimental investigation of runoff production in permeable soils. *Water Resour. Res.*, **6**, 478–490, doi:10.1029/WR006i002p00478.

——, and ——, 1970b: Partial area contributions to storm runoff in a small New England watershed. *Water Resour. Res.*, **6**, 1296–1311, doi:10.1029/WR006i005p01296.

Efstratiadis, A., and D. Koutsoyiannis, 2010: One decade of multi-objective calibration approaches in hydrological modelling: A review. *Hydrol. Sci. J.*, **55**, 58–78, doi:10.1080/02626660903526292.

Falge, E., and Coauthors, 2001: Gap filling strategies for long term energy flux data sets. *Agric. For. Meteor.*, **107**, 71–77, doi:10.1016/S0168-1923(00)00235-5.

Fan, Y., H. Li, and G. Miguez-Macho, 2013: Global patterns of groundwater table depth. *Science*, **339**, 940–943, doi:10.1126/science.1229881.

Fang, X., and J. Pomeroy, 2009: Modelling blowing snow redistribution to prairie wetlands. *Hydrol. Processes*, **23**, 2557–2569, doi:10.1002/hyp.7348.

Freeze, R. A., and J. A. Cherry, 1979: *Groundwater*. Prentice-Hall, 604 pp.

Gao, H., and Coauthors, 2009: Water budget record from Variable Infiltration Capacity (VIC) model. Algorithm Theoretical Basis Doc., 56 pp. [Available online at http://www.hydro.washington.edu/SurfaceWaterGroup/Publications/Water_Cycle_MEaSUREs_ATBD_VICmodel_submit.doc.]

Ghan, S., J. Liljegren, W. Shaw, J. Hubbe, and J. Doran, 1997: Influence of subgrid variability on surface hydrology. *J. Climate*, **10**, 3157–3166, doi:10.1175/1520-0442(1997)010<3157:IOSVOS>2.0.CO;2.

Gochis, D., W. Yu, and D. Yates, 2013: The WRF-Hydro model technical description and user's guide, version 1.0. NCAR Tech. Doc., 120 pp. [Available online at https://www.ral.ucar.edu/projects/wrf_hydro.]

Gupta, H. V., S. Sorooshian, and P. O. Yapo, 1998: Toward improved calibration of hydrologic models: Multiple and noncommensurable measures of information. *Water Resour. Res.*, **34**, 751–763, doi:10.1029/97WR03495.

——, L. Bastidas, S. Sorooshian, W. Shuttleworth, and Z. Yang, 1999: Parameter estimation of a land surface scheme using multicriteria methods. *J. Geophys. Res.*, **104**, 19 491–19 503, doi:10.1029/1999JD900154.

——, S. Sorooshian, T. S. Hogue, and D. P. Boyle, 2003: Advances in automatic calibration of watershed models. *Calibration of Watershed Models*, Q. Duan et al., Eds., Water Science and Application Series, Vol. 6, Amer. Geophys. Union, 9–28.

Habets, F., and Coauthors, 1999: The ISBA surface scheme in a macroscale hydrological model applied to the Hapex-Mobilhy area: Part I: Model and database. *J. Hydrol.*, **217**, 75–96, doi:10.1016/S0022-1694(99)00019-0.

Harbaugh, A. W., E. R. Banta, M. C. Hill, and M. G. McDonald, 2000: MODFLOW-2000, the US Geological Survey modular ground-water model—User guide to modularization concepts and the ground-water flow process. USGS Open-File Rep. 00-92, 121 pp. [Available online at https://pubs.usgs.gov/of/2000/0092/report.pdf.]

Harrison, K. W., S. V. Kumar, C. D. Peters-Lidard, and J. A. Santanello, 2012: Quantifying the change in soil moisture modeling uncertainty from remote sensing observations using Bayesian inference techniques. *Water Resour. Res.*, **48**, W11514, doi:10.1029/2012WR012337.

Henderson-Sellers, A., A. Pitman, P. Love, P. Irannejad, and T. Chen, 1995: The Project for Intercomparison of Land Surface Parameterization Schemes (PILPS): Phases 2 and 3. *Bull. Amer. Meteor. Soc.*, **76**, 489–503, doi:10.1175/1520-0477(1995)076<0489:TPFIOL>2.0.CO;2.

Hess, R., 2001: Assimilation of screen-level observations by variational soil moisture analysis. *Meteor. Atmos. Phys.*, **77**, 145–154, doi:10.1007/s007030170023.

Hogue, T. S., L. Bastidas, H. Gupta, S. Sorooshian, K. Mitchell, and W. Emmerich, 2005: Evaluation and transferability of the Noah land surface model in semiarid environments. *J. Hydrometeor.*, **6**, 68–84, doi:10.1175/JHM-402.1.

Hollinger, D., and A. Richardson, 2005: Uncertainty in eddy covariance measurements and its application to physiological models. *Tree Physiol.*, **25**, 873–885, doi:10.1093/treephys/25.7.873.

Horton, R. E., 1933: The role of infiltration in the hydrologic cycle. *Eos, Trans. Amer. Geophys. Union*, **14**, 446–460, doi:10.1029/TR014i001p00446.

Huang, M., Z. Hou, L. R. Leung, Y. Ke, Y. Liu, Z. Fang, and Y. Sun, 2013: Uncertainty analysis of runoff simulations and parameter identifiability in the Community Land Model: Evidence from MOPEX basins. *J. Hydrometeor.*, **14**, 1754–1772, doi:10.1175/JHM-D-12-0138.1.

Husain, S., N. Alavi, S. Bélair, M. Carrera, S. Zhang, V. Fortin, M. Abrahamowicz, and N. Gauthier, 2016: The multi-budget Soil, Vegetation, and Snow (SVS) scheme for land surface parameterization: Offline warm season evaluation. *J. Hydrometeor.*, doi:10.1175/JHM-D-15-0228.1, in press.

Ironside, G., 1991: Ecological land survey: Background and general approach. Guidelines for the integration of wildlife and habitat evaluations with ecological land survey, Environment Canada Tech. Rep., H. A. Stelfox, G. R. Ironside, and J. L. Kansas, Eds., 3–10. [Available online at http://agrienvarchive.ca/fed/download/wildlife_habitat_eval_ecol_land_surv91.pdf.]

Jajarmizadeh, M., S. Harun, and M. Salarpour, 2012: A review on theoretical consideration and types of models in hydrology. *J. Environ. Sci. Technol.*, **5**, 249, doi:10.3923/jest.2012.249.261.

Jones, N. E., 2010: Incorporating lakes within the river discontinuum: Longitudinal changes in ecological characteristics in stream–lake networks. *Can. J. Fish. Aquat. Sci.*, **67**, 1350–1362, doi:10.1139/F10-069.

Judd-Henrey, I., G. van der Kamp, M. Wismer, and A. Rodriguez-Prado, 2008: Assessment of ground and surface water conditions in the Prince Albert Model Forest Area. Saskatchewan Research Council Publication 11618-1E08, 47 pp.

Karvonen, T., H. Koivusalo, M. Jauhiainen, J. Palko, and K. Weppling, 1999: A hydrological model for predicting runoff from different land use areas. *J. Hydrol.*, **217**, 253–265, doi:10.1016/S0022-1694(98)00280-7.

Ke, Y., L. Leung, M. Huang, and H. Li, 2013: Enhancing the representation of subgrid land surface characteristics in land surface models. *Geosci. Model Dev.*, **6**, 1609–1622, doi:10.5194/gmd-6-1609-2013.

Klemeš, V., 1986: Operational testing of hydrological simulation models. *Hydrol. Sci. J.*, **31**, 13–24, doi:10.1080/02626668609491024.

Koster, R. D., M. J. Suarez, A. Ducharne, M. Stieglitz, and P. Kumar, 2000: A catchment-based approach to modeling land surface processes in a general circulation model: 1. Model structure. *J. Geophys. Res.*, **105**, 24 809–24 822, doi:10.1029/2000JD900327.

Kouwen, N., and S.-F. Mousavi, 2002: WATFLOOD/SPL9 hydrological model & flood forecasting system. *Mathematical Models of Large Watershed Hydrology*, V. P. Singh and D. K. Frevert, Eds., Water Resources Publications, 649–685.

Lawrence, D. M., and Coauthors, 2011: Parameterization improvements and functional and structural advances in version

4 of the Community Land Model. *J. Adv. Model. Earth Syst.*, **3**, M03001, doi:10.1029/2011MS00045.

Leavesley, G., and L. Stannard, 1990: Application of remotely sensed data in a distributed-parameter watershed model. *Applications of Remote Sensing in Hydrology*, G. Kite and A. Wankiewicz, Eds., NHRI, 47–64.

Liang, X., D. P. Lettenmaier, E. F. Wood, and S. J. Burges, 1994: A simple hydrologically based model of land surface water and energy fluxes for general circulation models. *J. Geophys. Res.*, **99**, 14 415–14 428, doi:10.1029/94JD00483.

——, E. F. Wood, and D. P. Lettenmaier, 1996: Surface soil moisture parameterization of the VIC-2L model: Evaluation and modification. *Global Planet. Change*, **13**, 195–206, doi:10.1016/0921-8181(95)00046-1.

Liu, Y., L. A. Bastidas, H. V. Gupta, and S. Sorooshian, 2003: Impacts of a parameterization deficiency on offline and coupled land surface model simulations. *J. Hydrometeor.*, **4**, 901–914, doi:10.1175/1525-7541(2003)004<0901:IOAPDO>2.0.CO;2.

——, H. V. Gupta, S. Sorooshian, L. A. Bastidas, and W. J. Shuttleworth, 2004: Exploring parameter sensitivities of the land surface using a locally coupled land–atmosphere model. *J. Geophys. Res.*, **109**, D21101, doi:10.1029/2004JD004730.

——, ——, ——, ——, and ——, 2005: Constraining land surface and atmospheric parameters of a locally coupled model using observational data. *J. Hydrometeor.*, **6**, 156–172, doi:10.1175/JHM407.1.

Livneh, B., Y. Xia, K. E. Mitchell, M. B. Ek, and D. P. Lettenmaier, 2010: Noah LSM snow model diagnostics and enhancements. *J. Hydrometeor.*, **11**, 721–738, doi:10.1175/2009JHM1174.1.

Lohmann, D., R. Nolte-Holube, and E. Raschke, 1996: A large-scale horizontal routing model to be coupled to land surface parametrization schemes. *Tellus*, **48A**, 708–721, doi:10.1034/j.1600-0870.1996.t01-3-00009.x.

——, E. Raschke, B. Nijssen, and D. Lettenmaier, 1998: Regional scale hydrology: I. Formulation of the VIC-2L model coupled to a routing model. *Hydrol. Sci. J.*, **43**, 131–141, doi:10.1080/02626669809492107.

MacDonald, M. K., 2010: Hydrological response unit-based blowing snow modelling over mountainous terrain. M.S. thesis, Dept. of Geography and Planning, University of Saskatchewan, 186 pp. [Available online at https://ecommons.usask.ca/handle/10388/etd-12202010-155704.]

——, J. W. Pomeroy, and A. Pietroniro, 2009: Parameterizing redistribution and sublimation of blowing snow for hydrological models: Tests in a mountainous subarctic catchment. *Hydrol. Processes*, **23**, 2570–2583, doi:10.1002/hyp.7356.

Mamo, M. T., 2015: Exploring the ability of a distributed hydrological land surface model in simulating hydrological processes in the boreal forest environment. M.S. thesis, Department of Civil and Geological Engineering, University of Saskatchewan, 153 pp.

Manabe, S., 1969: Climate and the ocean circulation: I. The atmospheric circulation and the hydrology of the earth's surface. *Mon. Wea. Rev.*, **97**, 739–774, doi:10.1175/1520-0493(1969)097<0739:CATOC>2.3.CO;2.

Marin, S., G. van der Kamp, A. Pietroniro, B. Davison, and B. Toth, 2010: Use of geological weighing lysimeters to calibrate a distributed hydrological model for the simulation of land–atmosphere moisture exchange. *J. Hydrol.*, **383**, 179–185, doi:10.1016/j.jhydrol.2009.12.034.

Matott, L. S., J. E. Babendreier, and S. T. Purucker, 2009: Evaluating uncertainty in integrated environmental models: A review of concepts and tools. *Water Resour. Res.*, **45**, W06421, doi:10.1029/2008WR007301.

Maxwell, R. M., and S. J. Kollet, 2008: Interdependence of groundwater dynamics and land-energy feedbacks under climate change. *Nat. Geosci.*, **1**, 665–669, doi:10.1038/ngeo315.

McDonnell, J. J., 2003: Where does water go when it rains? Moving beyond the variable source area concept of rainfall–runoff response. *Hydrol. Processes*, **17**, 1869–1875, doi:10.1002/hyp.5132.

——, 2013: Are all runoff processes the same? *Hydrol. Processes*, **27**, 4103–4111, doi:10.1002/hyp.10076.

——, and Coauthors, 2007: Moving beyond heterogeneity and process complexity: A new vision for watershed hydrology. *Water Resour. Res.*, **43**, W07301, doi:10.1029/2006WR005467.

Mekonnen, M., H. Wheater, A. Ireson, C. Spence, B. Davison, and A. Pietroniro, 2014: Towards an improved land surface scheme for prairie landscapes. *J. Hydrol.*, **511**, 105–116, doi:10.1016/j.jhydrol.2014.01.020.

Mendoza, P. A., M. P. Clark, M. Barlage, B. Rajagopalan, L. Samaniego, G. Abramowitz, and H. Gupta, 2015: Are we unnecessarily constraining the agility of complex process-based models? *Water Resour. Res.*, **51**, 716–728, doi:10.1002/2014WR015820.

Miguez-Macho, G., and Y. Fan, 2012a: The role of groundwater in the Amazon water cycle: 1. Influence on seasonal streamflow, flooding and wetlands. *J. Geophys. Res.*, **117**, D15113, doi:10.1029/2012JD017539.

——, and ——, 2012b: The role of groundwater in the Amazon water cycle: 2. Influence on seasonal soil moisture and evapotranspiration. *J. Geophys. Res.*, **117**, D15114, doi:10.1029/2012JD017540.

Mingelbier, M., P. Brodeur, and J. Morin, 2008: Spatially explicit model predicting the spawning habitat and early stage mortality of northern pike (*Esox lucius*) in a large system: The St. Lawrence River between 1960 and 2000. *Hydrobiologia*, **601**, 55–69, doi:10.1007/s10750-007-9266-z.

Mitchell, K., 2005: The community Noah land-surface model (LSM) user's guide, version 2.7.1. NOAA/NCEP Doc., 26 pp. [Available online at ftp://ftp.emc.ncep.noaa.gov/mmb/gcp/ldas/noahlsm/ver_2.7.1.]

Moncrieff, J. B., and Coauthors, 1997: A system to measure surface fluxes of momentum, sensible heat, water vapour and carbon dioxide. *J. Hydrol.*, **188–189**, 589–611, doi:10.1016/S0022-1694(96)03194-0.

Morgenstern, K., and Coauthors, 2004: Sensitivity and uncertainty of the carbon balance of a Pacific Northwest Douglas-fir forest during an El Niño/La Niña cycle. *Agric. For. Meteor.*, **123**, 201–219, doi:10.1016/j.agrformet.2003.12.003.

Moriasi, D., J. Arnold, M. Van Liew, R. Bingner, R. Harmel, and T. Veith, 2007: Model evaluation guidelines for systematic quantification of accuracy in watershed simulations. *Trans. ASABE*, **50**, 885–900, doi:10.13031/2013.23153.

Morin, J., O. Champoux, M. Mingelbier, J. A. Bechara, Y. Secretan, M. Jean, and J.-J. Frenette, 2003: Emergence of new explanatory variables for 2D habitat modelling in large rivers: The St. Lawrence experience. *Can. Water Resour. J.*, **28**, 249–272, doi:10.4296/cwrj2802249.

Nash, J., and J. Sutcliffe, 1970: River flow forecasting through conceptual models part I—A discussion of principles. *J. Hydrol.*, **10**, 282–290, doi:10.1016/0022-1694(70)90255-6.

Nasonova, O. N., Y. M. Gusev, and Y. E. Kovalev, 2009: Investigating the ability of a land surface model to simulate streamflow with the accuracy of hydrological models: A case study using MOPEX materials. *J. Hydrometeor.*, **10**, 1128–1150, doi:10.1175/2009JHM1083.1.

Natural Resources Canada, 2007: Canadian Digital Elevation Data, level 1 product specifications. NRC Doc., 48 pp.

[Available online at http://ftp2.cits.rncan.gc.ca/pub/geobase/official/cded/doc/GeoBase_product_specs_CDED1_en.pdf.]

——, 2015: Land cover, circa 2000—Vector. NRC Doc., 7 pp. [Available online at http://wmsmir.cits.rncan.gc.ca/index.html/pub/geobase/official/lcc2000v_csc2000v/doc/Land_Cover.pdf.]

Nazemi, A., and H. Wheater, 2015a: On inclusion of water resource management in Earth system models—Part 1: Problem definition and representation of water demand. *Hydrol. Earth Syst. Sci.*, **19**, 33–61, doi:10.5194/hess-19-33-2015.

——, and ——, 2015b: On inclusion of water resource management in Earth system models—Part 2: Representation of water supply and allocation and opportunities for improved modeling. *Hydrol. Earth Syst. Sci.*, **19**, 63–90, doi:10.5194/hess-19-63-2015.

Neumann, N., and P. Marsh, 1998: Local advection of sensible heat in the snowmelt landscape of arctic tundra. *Hydrol. Processes*, **12**, 1547–1560, doi:10.1002/(SICI)1099-1085(199808/09)12:10/11<1547::AID-HYP680>3.0.CO;2-Z.

Nijssen, B., and D. P. Lettenmaier, 2002: Water balance dynamics of a boreal forest watershed: White Gull Creek basin, 1994–1996. *Water Resour. Res.*, **38**, 1255, doi:10.1029/2001WR000699.

Niu, G.-Y., and X. Zeng, 2012: Earth system model, modeling the land component of. *Climate Change Modeling Methodology*, P. J. Rasch, Ed., Springer, 139–168, doi:10.1007/978-1-4614-5767-1_7.

——, Z.-L. Yang, R. E. Dickinson, and L. E. Gulden, 2005: A simple TOPMODEL-based runoff parameterization (SIMTOP) for use in global climate models. *J. Geophys. Res.*, **110**, D21106, doi:10.1029/2005JD006111.

——, and Coauthors, 2011: The community Noah land surface model with multiparameterization options (Noah-MP): 1. Model description and evaluation with local-scale measurements. *J. Geophys. Res.*, **116**, D12109, doi:10.1029/2010JD015139.

Oleson, K. W., and Coauthors, 2010: Technical description of version 4.0 of the Community Land Model (CLM). NCAR Tech. Note NCAR/TN-478+STR, 257 pp., doi:10.5065/D6FB50WZ.

ORNL DAAC, 2015: FLUXNET web page. Accessed 13 June 2016. [Available online at http://fluxnet.ornl.gov.]

Pappenberger, F., H. Cloke, G. Balsamo, T. Ngo-Duc, and T. Oki, 2010: Global runoff routing with the hydrological component of the ECMWF NWP system. *Int. J. Climatol.*, **30**, 2155–2174, doi:10.1002/joc.2028.

Peters-Lidard, C. D., D. M. Mocko, M. Garcia, J. A. Santanello, M. A. Tischler, M. S. Moran, and Y. Wu, 2008: Role of precipitation uncertainty in the estimation of hydrologic soil properties using remotely sensed soil moisture in a semiarid environment. *Water Resour. Res.*, **44**, W05S18, doi:10.1029/2007WR005884.

Pietroniro, A., and Coauthors, 2007: Development of the MESH modelling system for hydrological ensemble forecasting of the Laurentian Great Lakes at the regional scale. *Hydrol. Earth Syst. Sci.*, **11**, 1279–1294, doi:10.5194/hess-11-1279-2007.

Pitman, A., 2003: The evolution of, and revolution in, land surface schemes designed for climate models. *Int. J. Climatol.*, **23**, 479–510, doi:10.1002/joc.893.

Pokhrel, Y., N. Hanasaki, S. Koirala, J. Cho, P. J.-F. Yeh, H. Kim, S. Kanae, and T. Oki, 2012: Incorporating anthropogenic water regulation modules into a land surface model. *J. Hydrometeor.*, **13**, 255–269, doi:10.1175/JHM-D-11-013.1.

Price, J., and J. Waddington, 2000: Advances in Canadian wetland hydrology and biogeochemistry. *Hydrol. Processes*, **14**, 1579–1589, doi:10.1002/1099-1085(20000630)14:9<1579::AID-HYP76>3.0.CO;2-#.

Reed, P. M., D. Hadka, J. D. Herman, J. R. Kasprzyk, and J. B. Kollat, 2013: Evolutionary multiobjective optimization in water resources: The past, present, and future. *Adv. Water Resour.*, **51**, 438–456, doi:10.1016/j.advwatres.2012.01.005.

Rogers, R. R., and M. Yau, 1989: *A Short Course in Cloud Physics*. 3rd ed. International Series in Natural Philosophy, Vol. 113, Butterworth Heinemann, 304 pp.

Samaniego, L., R. Kumar, and S. Attinger, 2010: Multiscale parameter regionalization of a grid-based hydrologic model at the mesoscale. *Water Resour. Res.*, **46**, W05523, doi:10.1029/2008WR007327.

Santanello, J. A., Jr., C. D. Peters-Lidard, M. E. Garcia, D. M. Mocko, M. A. Tischler, M. S. Moran, and D. Thoma, 2007: Using remotely-sensed estimates of soil moisture to infer soil texture and hydraulic properties across a semi-arid watershed. *Remote Sens. Environ.*, **110**, 79–97, doi:10.1016/j.rse.2007.02.007.

——, ——, A. Kennedy, and S. V. Kumar, 2013: Diagnosing the nature of land–atmosphere coupling: A case study of dry/wet extremes in the U.S. Southern Great Plains. *J. Hydrometeor.*, **14**, 3–24, doi:10.1175/JHM-D-12-023.1.

Schaake, J. C., V. I. Koren, Q.-Y. Duan, K. Mitchell, and F. Chen, 1996: Simple water balance model for estimating runoff at different spatial and temporal scales. *J. Geophys. Res.*, **101**, 7461–7475, doi:10.1029/95JD02892.

Schottler, S. P., J. Ulrich, P. Belmont, R. Moore, J. Lauer, D. R. Engstrom, and J. E. Almendinger, 2014: Twentieth century agricultural drainage creates more erosive rivers. *Hydrol. Processes*, **28**, 1951–1961, doi:10.1002/hyp.9738.

Sellers, P. J., and Coauthors, 1997a: Modeling the exchanges of energy, water, and carbon between continents and the atmosphere. *Science*, **275**, 502–509, doi:10.1126/science.275.5299.502.

——, and Coauthors, 1997b: Boreas in 1997: Experiment overview, scientific results, and future directions. *J. Geophys. Res.*, **102**, 28 731–28 769, doi:10.1029/97JD03300.

Soulis, E. D., and F. R. Seglenieks, 2008: The MAGS integrated modeling system. *Hydrologic Processes*, Vol. 2, *Cold Region Atmospheric and Hydrologic Studies: The Mackenzie GEWEX Experience*, Springer, 445–473, doi:10.1007/978-3-540-75136-6_24.

——, K. Snelgrove, N. Kouwen, F. Seglenieks, and D. Verseghy, 2000: Towards closing the vertical water balance in Canadian atmospheric models: Coupling of the land surface scheme CLASS with the distributed hydrological model WATFLOOD. *Atmos.–Ocean*, **38**, 251–269, doi:10.1080/07055900.2000.9649648.

——, J. Craig, V. Fortin, and G. Liu, 2011: A simple expression for the bulk field capacity of a sloping soil horizon. *Hydrol. Processes*, **25**, 112–116, doi:10.1002/hyp.7827.

Spence, C., 2010: A paradigm shift in hydrology: Storage thresholds across scales influence catchment runoff generation. *Geogr. Compass*, **4**, 819–833, doi:10.1111/j.1749-8198.2010.00341.x.

Takata, K., S. Emori, and T. Watanabe, 2003: Development of the minimal advanced treatments of surface interaction and runoff. *Global Planet. Change*, **38**, 209–222, doi:10.1016/S0921-8181(03)00030-4.

Taylor, R. G., and Coauthors, 2013: Ground water and climate change. *Nat. Climate Change*, **3**, 322–329, doi:10.1038/nclimate1744.

Todini, E., 1988: Rainfall–runoff modeling—Past, present and future. *J. Hydrol.*, **100**, 341–352, doi:10.1016/0022-1694(88)90191-6.

Tolson, B. A., and C. A. Shoemaker, 2007: Dynamically dimensioned search algorithm for computationally efficient watershed model calibration. *Water Resour. Res.*, **43**, W01413, doi:10.1029/2005WR004723.

van der Kamp, G., and M. Hayashi, 2009: Groundwater–wetland ecosystem interaction in the semiarid glaciated plains of North America. *Hydrogeol. J.*, **17**, 203–214, doi:10.1007/s10040-008-0367-1.

Vergnes, J.-P., B. Decharme, R. Alkama, E. Martin, F. Habets, and H. Douville, 2012: A simple groundwater scheme for hydrological and climate applications: Description and offline evaluation over France. *J. Hydrometeor.*, **13**, 1149–1171, doi:10.1175/JHM-D-11-0149.1.

Verseghy, D., 1991: CLASS—A Canadian land surface scheme for GCMs. I. Soil model. *Int. J. Climatol.*, **11**, 111–133, doi:10.1002/joc.3370110202.

——, 2011: CLASS—The Canadian land surface scheme (version 3.5): Technical documentation (version 1). Environment Canada, 180 pp.

——, N. McFarlane, and M. Lazare, 1993: CLASS—A Canadian land surface scheme for GCMs. II. Vegetation model and coupled runs. *Int. J. Climatol.*, **13**, 347–370, doi:10.1002/joc.3370130402.

Vionnet, V., E. Martin, V. Masson, G. Guyomarc'h, F. N. Bouvet, A. Prokop, Y. Durand, and C. Lac, 2014: Simulation of wind-induced snow transport and sublimation in alpine terrain using a fully coupled snowpack/atmosphere model. *Cryosphere*, **8**, 395–415, doi:10.5194/tc-8-395-2014.

Voisin, N., H. Li, D. Ward, M. Huang, M. Wigmosta, and L. Leung, 2013a: On an improved sub-regional water resources management representation for integration into Earth system models. *Hydrol. Earth Syst. Sci.*, **17**, 3605–3622, doi:10.5194/hess-17-3605-2013.

——, L. Liu, M. Hejazi, T. Tesfa, H. Li, M. Huang, Y. Liu, and L. Leung, 2013b: One-way coupling of an integrated assessment model and a water resources model: Evaluation and implications of future changes over the US Midwest. *Hydrol. Earth Syst. Sci.*, **17**, 4555–4575, doi:10.5194/hess-17-4555-2013.

Weiler, M., J. J. McDonnell, I. Tromp-van Meerveld, and T. Uchida, 2005: Subsurface stormflow. *Rainfall–Runoff Processes*, Part 10, *Encyclopedia of Hydrological Sciences*, M. G. Anderson, Ed., Wiley, 112.

Wood, E. F., and Coauthors, 2011: Hyperresolution global land surface modeling: Meeting a grand challenge for monitoring Earth's terrestrial water. *Water Resour. Res.*, **47**, W05301, doi:10.1029/2010WR010090.

Xie, Z., F. Yuan, Q. Duan, J. Zheng, M. Liang, and F. Chen, 2007: Regional parameter estimation of the VIC land surface model: Methodology and application to river basins in China. *J. Hydrometeor.*, **8**, 447–468, doi:10.1175/JHM568.1.

Yang, Z.-L., 2004: Modeling land surface processes in short-term weather and climate studies. Observation, *Theory and Modeling of Atmospheric Variability*, X. Zhu et al., Eds., World Scientific Series on Asia-Pacific Weather and Climate, Vol. 3, World Scientific, 288–313, doi:10.1142/9789812791139_0014.

Zulkafli, Z., W. Buytaert, C. Onof, W. Lavado, and J.-L. Guyot, 2013: A critical assessment of the JULES land surface model hydrology for humid tropical environments. *Hydrol. Earth Syst. Sci.*, **17**, 1113–1132, doi:10.5194/hess-17-1113-2013.